# Aesculap Neurosurgery
## MINOP® TREND

Endoscopic transsphenoidal surgery
of the central skull base


**Robert Reisch**

In collaboration with
Gábor Baksa and Lajos Patonay


B|BRAUN
SHARING EXPERTISE

MINOP®
TREND

# The endonasal transsphenoidal biportal binostril approach

**The TREND pituitary endoscope**
**A trend-setting equipment for transsphenoidal endoscopic exposure of the pituitary gland and surrounding structures**

B|BRAUN
SHARING EXPERTISE

# Preface


Robert Reisch

Head of the Division Minimally Invasive Endoscopic Neurosurgery
Department of Neurosurgery
University Hospital Zurich, Switzerland
Chairman: Helmut Bertalanffy

In collaboration with
Gábor Baksa & Lajos Patonay
Laboratory of Applied and Clinical Anatomy
Semmelweis University Budapest, Hungary

Illustrations and Layout
Stefan Kindel
Maikammer, Germany


**Keyhole Approaches in Neurosurgery**
**Volume 1: Concept and Surgical Technique**

*Axel Perneczky, Robert Reisch*

In collaboration with Manfred Tschabitscher
Illustrated by Stefan Kindel
With a foreword by Tetsuo Kanno


Springer Verlag Wien, 2008

ISBN: 978-3-211-83885-3


The enormous technological development in and around the modern neurosurgery with high sophisticated preoperative imaging of the individual pathoanatomical situation, tailored planning of the operative procedure, routinely application of neuronavigation devices and the intraoperative use of endoscopes enable neurosurgeons to perform limited keyhole approaches, minimizing the surgery related intraoperative traumatization.

In this publication the authors offer a systematic overview on minimally invasive approaches. In the first volume entitled "Keyhole Approaches in Neurosurgery. Concept and Surgical Technique", different minimally invasive craniotomies are described in detail. After depiction of the historical development, concept and technique of minimally invasive neurosurgery, each chapter illustrates a particular keyhole approach in a comprehensive way. The surgical approach and the anatomical construction of the target region are illustrated using artistic illustrations and photographs on human cadaver dissections. Concentrating on surgical practice, patient positioning, anatomical orientation, the stages of the surgical approach, potential errors with their consequences and important tips and tricks are discussed in detail, providing instructions for everyday use.

In the second volume with the title "Keyhole Approaches in Neurosurgery. Illustrative Cases", scheduled to appear in 2009, the authors present expressive operative cases demonstrating the practical application of these keyhole approaches. The cases represent skull base tumors and vascular lesions – each of them leads to extended discussion on the possible surgical solution treating in consensus of minimally invasive keyhole strategy.

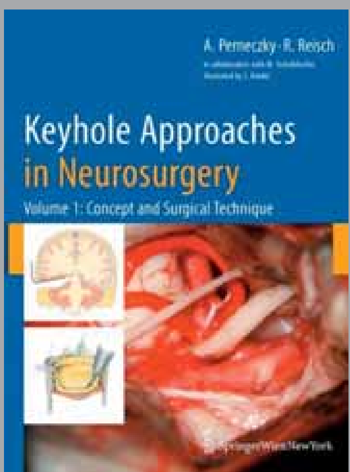

MINOP®
TREND

# The endonasal transsphenoidal biportal binostril approach

The TREND pituitary endoscope
A trend-setting equipment for transsphenoidal endoscopic exposure of the pituitary gland and surrounding structures

When looking at recent publications on transsphenoidal surgery, it will be clear that TRanssphenoidal ENDoscopy is TREND-setting! However, this endoscopic technique is not in routine use everywhere and neurosurgeons are often reluctant to use it: one is often cautious about an endoscopic endonasal dissection because the permanent contamination of the endoscope with blood and nasal secretions hinders orientation. In addition, the para-endoscopic and biportal dissection is very unfamiliar requiring an unacceptably steep learning curve. The first frustrating steps add to the growing impatience of surgeons who then go no further!

Nevertheless, endoscopic visualization and para-endoscopic dissection without using the surgical microscope offers several undisputable advantages.

Advantages in visualization are the increased light intensity in the deep-seated surgical field and the clear representation of patho-anatomical details. In addition, the extended viewing angle of endoscopes enables surgeons to observe hidden parts of the surgical field. The major benefit in surgical dissection is the unhindered approach to these clearly visible structures: without using a nasal speculum, surgical manipulation is not impeded and the instruments are freely mobile. In addition, a pure endoscopic technique avoids the need for rhinoseptal submucosal dissection providing a direct and quicker approach to the sphenoid sinus. The method avoids the need for postoperative nasal packing, thus causing less pain and discomfort after surgery, providing better nasal airflow and a shorter hospital stay.

In this brochure, we wish to provide effective assistance in introducing the endoscopic technique into the daily routine treatment of sellar and parasellar lesions via the transsphenoidal route. After a short historical background, the anatomy of the nasal cavity and the supra- and parasellar regions is illustrated focusing on an endoscopically adapted and applied description. The technique of the endosnasal transsphenoidal biportal-binostril approach is described in detail with illustrative cases.

The conclusion consists of a comprehensive description of the AESCULAP TREND pituitary endoscope system with a configuration of newly developed instruments especially designed for transsphenoidal endoscopic surgery.

Robert Reisch

# Statements

"Well done! This manual nicely summarize the history as well as conventional and endoscopic anatomy of transsphenoidal surgery. In addition, the endonasal biportal approach is demonstrated in detail including the specific setting in the OR and is augmented with 3 illustrative cases. It becomes very obvious, that the MINOP TREND is a mature and sophisticated endoscopy system really based on neurosurgeons necessities and designed not only for standard pituitary surgery but also advanced transsphenoidal endoscopic surgery of the skull base. The manual is extremely valuable for the beginner providing all basic knowledge to get things going as well as for the experienced user by demonstrating important tips and tricks. Having had the opportunity to use this system myself, I was impressed by the brilliant and bright image, easy and intuitive handling, and outstanding flexibility of the system by means of being able to use it also conveniently with a holding device. The latter makes it extremely useful for extended endoscopic skull base surgery. Based on my personal experience I can recommend the MINOP TREND system without any restrictions and like to congratulate the authors for this beautiful and illustrative manual, which makes transsphenoidal surgery much easier."

*Nikolai J. Hopf*
*Stuttgart, Germany*

"Endoscopic transsphenoidal surgery has advanced significantly within the last years and will continue to do so in the future. Despite of all controversies in regard of indication and surgical technique, the experience has shown that the utilization of an endoscope provides excellent visualization and therefore orientation within the sphenoid sinus, the sella and surrounding structures.
The MINOP TREND system has been developed in close cooperation among the Aesculap company and the potential users, neurosurgeons from Europe, Australia and the United States. This has lead to further improvement compared to existing systems, especially in the ergonomic handling of the endoscope and the use of instruments, either in two-hand or four-hand technique.
The manual was written by Prof. Robert Reisch, one of the most experienced and well recognized Endoscopic and skull base surgeons in Germany. It reflects the concept of the TREND very well; it's a pragmatic tool for further improvement in patient care."

*Michael J. Fritsch*
*Greifswald, Germany*

"Dr. Reisch has created a superb and contemporary manual for endoscopic-assisted transsphenoidal skull base surgery. His historical review, anatomical descriptions, and easy to understand surgical outline should serve as an essential reference for any neurosurgeon or otolaryngologist intending to perform transnasal skull base surgery. Rarely are illustrations as clear and well marked as those provided in this manual by Dr. Reich. I particularly found the partitioned surgical steps practical. Additionally his introduction to the endoscopic system, the Aesculap TREND, is very useful and confirms the need for systems designed exclusively for transnasal surgery. I will personally reference this work to the many students and practicing neurosurgeons interested in applying minimally invasive technology into their repertoire."

*Mark M. Souweidane*
*New York, New York*

" In the operating manual on endoscopic transsphenoidal surgery of the central skull base Robert Reisch describes his experience with the biportal binostril approach as compared to t he more widely used mononostril exposure of the sellar region. I can only fully agree with his description of the advantages of the binostril approach since it is the exact technique that I have used since 1994. The manual is comprehensive but yet concise with extensive and beautiful illustrations for every single step of the procedure which is very helpful for the novice endoscopic neurosurgeon but also valuable for the more experienced ones. The final case illustration nicely shows the use of the new TREND system, that is explained in detail at the end. This manual will be of great value for everyone involved in endoscopic surgery of the skull base and I congratulate Robert Reisch with this excellent manuscript. "

*André Grotenhuis*
*Nijmegen, Netherlands*

" This illustrated compendium of the Endoscopic Transsphenoidal Surgery of the Central Skull Base is a concise and well illustrated manual for the use of transsphenoidal instrumentation for the pituitary fossa and the surrounding skull base.
The anatomy of the nasal cavity and the epipharynx as well as the anatomy for approaching the sphenoid sinus, parasellar region and skull base using endoscopic techniques is nicely illustrated. Particularly well illustrated is the endoscopic anatomy of the nasal cavity and sellar region with photographs of the basic approach to the sphenoid sinus using the endoscope.
Some surgeons are in favor of the biportal approach and this is well documented and discussed. The last chapter summarizes the use of the instrumentation and the TREND system by Aesculap. The biportal system is aided by the use of the holding arm.
All in all, this is a very comprehensive and well illustrated guide for the use of the TREND system in endoscopic transsphenoidal surgery of the central skull base. It is also a valuable compendium of anatomy and basic approaches to the pituitary fossa and expanded skull base that will be useful to any Neurosurgeon who focuses on this area. "

*Walter Grand*
*Buffalo, New York*

# Introduction

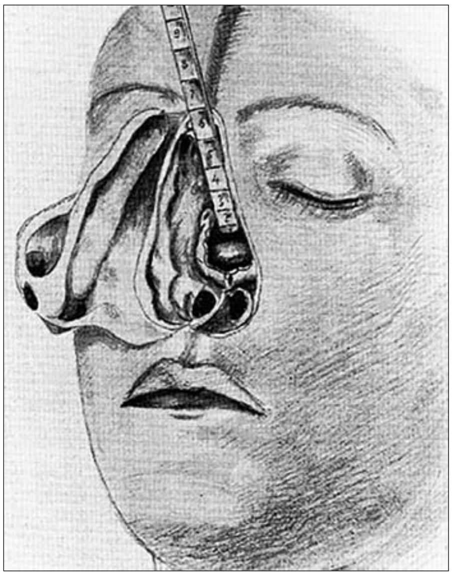

**Fig. 1** *Hermann Schloffer's transnasal macro-surgical approach described in 1907. Note the traumatic exposure for removal of an extended pituitary adenoma. To overcome the limited visibility, Schloffer used a stick to measure the depth and to palpate the tumor tissue.*

**Fig. 2** *Harvey Cushing, operating via a sub-labial – transnasal approach in 1923. Note the head-mounted lamp and the use of specially designed instruments.*

Transsphenoidal surgery for removal of a space-occupying pituitary tumor was first performed in 1907 by Hermann Schloffer in Innsbruck, Austria. In order to expose the central skull base, Schloffer had to use a broad approach: after a perinasal skin incision, he removed the nasal septum, all turbinates and the ethmoid bone with the medial orbital wall on both sides (Fig. 1).

Today, it is quite impossible to imagine that Schloffer dissected almost blindly within the deep-seated field without any illumination or magnification tools and using a stick for palpation of the tumor tissue. However the evolution of preoperative diagnostic tools, neurosurgical instruments and intraoperative illumination devices resulted in a major development in neurosurgical techniques making such interventions less dangerous and less traumatizing. In 1923, Harvey Cushing could report on a less disturbing technique using self-made instruments and a head-mounted lamp for his transsphenoidal macro-surgical approach (Fig. 2). Using this method, Cushing demonstrated a marked improvement in postoperative morbidity and mortality.

The real revolution in illumination of the surgical field, was, however, the introduction of operating microscopes in the 1960's and early 1970's. Dwight Parkinson, one of the real pioneers of microneurosurgery, pointed out very clearly the advantages of this new device: "...the neurosurgical section borrowed an operative microscope from the otolaryngology department. The microscope provided us with the enormous advantages of coaxial illumination, magnification, and simultaneous viewing for the surgeon and resident". The first neurosurgeon to use an operating microscope for transsphenoidal surgery was Jules Hardy in 1962. In the classic publication "Microneurosurgey. Applied to Neurosurgery", edited by M. Gazi Yasargil in 1969, Hardy reported on details of the technique having performed several operations with improved surgical effectiveness and safety (Fig. 3).

It is interesting to note that despite the enormous development in preoperative diagnostics, microneurosurgical techniques, illumination devices and microscopes, transsphenoidal surgery has not demonstrated a marked improvement since Hardy's first description. Gold standard is the transseptal exposure of the sphenoid sinus with sublabial or septal incision of the mucosa. However, the microsurgical transsphenoidal approach creates several different drawbacks during the procedure such as a) the predefined surgical corridor, b) narrow viewing angles with an almost coaxial control of the microinstruments, and c) reduction of light intensity in the deep-seated operating field with subsequently decreased intraoperative orientation (Fig. 4).

a) Due to the predefined surgical pathway given by the nasal speculum, the corridor of dissection cannot be changed during surgery; the narrow space between the blades of the speculum causes an almost coaxial view of the instruments and an distinct lack of free manipulation within the deep-seated field.

b) The eyes of the neurosurgeon must be able to see anatomical structures to save them and to recognize pathologies to attack them. The second main difficulty of microsurgical transsphenoidal approaches is the loss of intraoperative light and sight through the long and narrow surgical pathway, causing significantly reduced optical control during surgery. For the purpose of bringing light into the surgical field and controlling microinstruments with an adequate magnification, surgical microscopes can be effectively supplemented by the optical properties of modern endoscopes. The three advantages of endoscopes are as follows: 1) increased light intensity, 2) clear depiction of details in close-up positions, and 3) extended viewing angle.

c) This possibility of extended visualization solves the third and main problem of the microsurgical technique, namely the limited control of tumor removal in hidden parts of the surgical field. The view through the operating microscope allows a purely coaxial visualization; laterally located structures

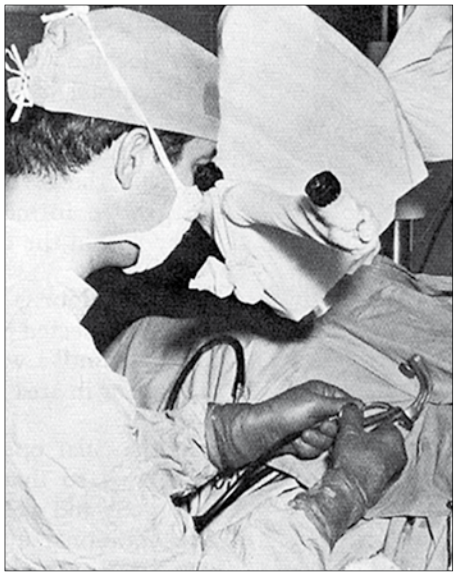

**Fig. 3** *Jules Hardy undertaking transnasal surgery using a first-generation operating microscope and C-arm for appropriate intraoperative orientation. Despite the enormous development in preoperative diagnostics, microneurosurgical techniques, illumination devices and microscopes, transsphenoidal surgery has not shown a marked improvement since Hardy's first description in 1962.*

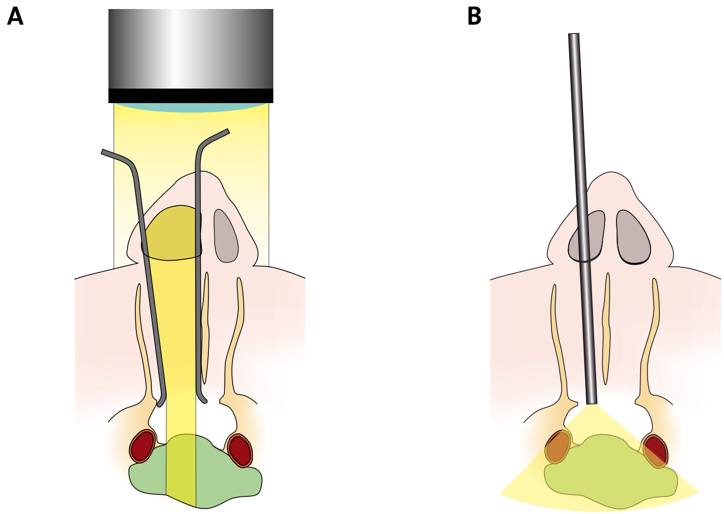


**Fig. 4 A** *Schematic drawing demonstrating a transsphenoidal exposure using operating microscope. Note that the technique creates significant drawbacks during the procedure. Due to the narrow and predefined surgical corridor given by the nasal speculum, visual control of tumor removal in hidden parts of the surgical field is extremely limited.*

**Fig. 4 B** *Endoscopic transsphenoidal exposure offering increased visibility. The improved light intensity, clear depiction of pathoanatomical details, and extended viewing angle ensure safe surgical dissection in the deep operating field and enable visually controlled tumor removal in hidden parts of the surgical field.*

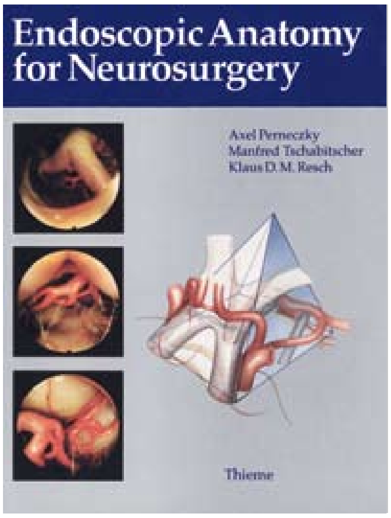


**Fig. 5** *In 1993, Axel Perneczky, Manfred Tschabitscher and Klaus D. M. Resch have published a comprehensive book on "Endoscopic Anatomy for Neurosurgery".*

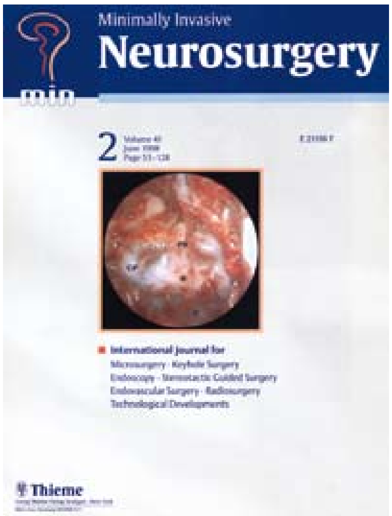


**Fig. 6** *In this issue of the pioneering journal "Minimally Invasive Neurosurgery" from 1998, Paolo Cappabianca and coworkers have reported the first experiences in endoscopic transnasal surgery.*

are concealed behind the nasal speculum resulting in uncontrolled surgery. However, blind tumor removal is compared with a higher risk of iatrogenic damage to neurovascular structures and with a possible increase in tumor remnants. With the intraoperative use of endoscopes, these laterally located parts of the field are visible and therefore surgically approachable.

The first surgeons who realized the limitations of visualization in transcranial surgery were Werner Prott in 1974 performing diagnostic endoscopic cisternoscopy of the cerebellopontine angle, Michael L. J. Apuzzo in 1977 when he introduced the so-called side-viewing telescope, and Frank Oppel in 1981 who used intraoperative endoscopy during microvascular trigeminal decompression. All of these descriptions can be regarded as the initiation of endoscope-assisted microneurosurgery, which, along with other neuroendoscopic techniques, experienced a revival in the 1990's. Innovators of the endoscope-assisted technique are Takanori Fukushima and Axel Perneczky who have published several fundamental papers on this topic (Fig. 5).

The true pioneer of endoscopy of the nasal cavity was Walter Messerklinger, founder of the technique of systematic endoscopic investigation of the nasal and paranasal cavities. The school in Graz, Austria with his student and later chairman Heinz Stammberger, developed the technique of functional endoscopic sinus surgery. The first attempt to use an endoscope for transsphenoidal pituitary surgery was in 1963 when Gérard Giuot supplemented the microsurgical exploration of the sellar region with an endoscope-assisted technique.

Recently, due to great advances in otorhinolaryngological and neurosurgical endoscopy, Guiot's basic idea has been reconsidered using the method of "pure endoscopy" in transsphenoidal pituitary surgery.

The initial publications on the pure endoscopic method described transnasal surgery of the pituitary gland. Hae Dong Jho reported his initial experience in 1996 and Paolo Cappabianca and Enrico de Divitiis in 1998 (Fig. 6). Nevertheless, within the last few years, several groups have dealt with extended endoscopic approaches exposing intracranial lesions via the transsphenoidal route. The teams of Capabianca and de Diviitis in Naples and David Locatelli and Paolo Castelnuovo in Pavia and the groups of Theodore Schwartz in New York and Amin Kassam in Pittsburgh have recently described the removal of extended intracranial pathologies using an endoscopic transsphenoidal technique.

# Anatomical background

The basis of minimizing damage within the surgical field is an anatomical understanding of the nasal and parasellar regions combined with special endoscopic experience. An essential step in basic endoscopic training is to identify anatomical landmarks with the special visualization technique and use them for appropriate surgical orientation. Thus, the path to transnasal endoscopic surgery leads through an anatomical-endoscopic laboratory with intensive use of cadavers. This training ensures not only safe dissection during the first surgically treated cases, but may shorten the initial steep learning curve.

**The nasal cavity and epipharynx**

The entrance to the nasal cavity is a pear-shaped opening bordered by the nasal and the maxillary frontal processes (Fig. 7). The piriform aperture is separated by the nasal septum, an osteocartilaginous and mucous formation with two mostly asymmetrical parts.

The nasal cavity itself is similar in configuration to the piriform aperture offering more space for surgical dissection in the basal part of the chamber (Fig. 8).

**Fig. 7** *The bony anterior aperture of the nasal cavity. Note the bordering nasal and maxillary bones and the osseous nasal septum. In several cases, severe alterations of the septum can hinder intranasal exploration.*

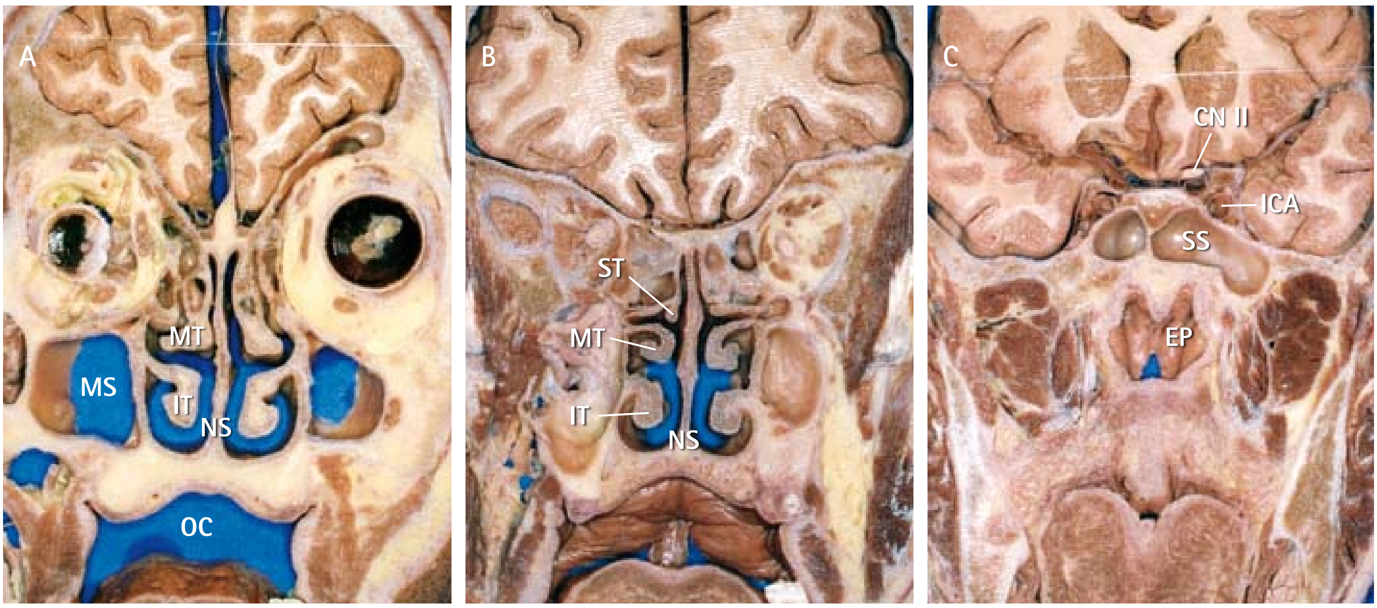


**Fig. 8** *Coronar sections in a fixed specimen in the anterior (A), middle (B) and posterior (C) portion of the skull base from an anterior view. The nasal cavity itself is similar in configuration to the piriform aperture offering more space for surgical dissection in the basal part of the chamber. Note the nasal septum and the highly irregular and variegated lateral wall of the nasal cavity. The posterior section (C) shows the sphenoid sinus and epipharynx.*

The floor of the nasal cavity comprises the maxillary palatine process and the horizontal palatine bone lamina; the medial wall is formed by the septum according to the perpendicular plate of the ethmoid, vomer and, near to the nostril, the quadrangular cartilage. The septum is bordered posterosuperiorly by the body of the sphenoid, following along the free edge of the vomer, at the choana. The narrow superior wall of the nasal cavity corresponds to the cribriform plate of the ethmoid bone (Figs. 8, 9).

The lateral wall is the most complex, forming a highly irregular and variegated anatomy. Six bones are involved: the maxillary, lacrimal, ethmoid, sphenoid and palatine bones and the inferior nasal turbinate (Fig. 10). The anterior part is created by the compact and thick frontal process of the maxilla and by the nasal bone. The posterior part is similarly stabilized by the maxillopalatine junction bordering the pterygopalatine fossa anteromedially. Here, in the upper part, is the sphenopalatine foramen, an important neurovascular connection of the pterygopalatine fossa to the nasal cavitiy.

**Fig. 9** *Paramedian sagittal sections showing the nasal septum in osseous (A) and fixed (B) specimens.*


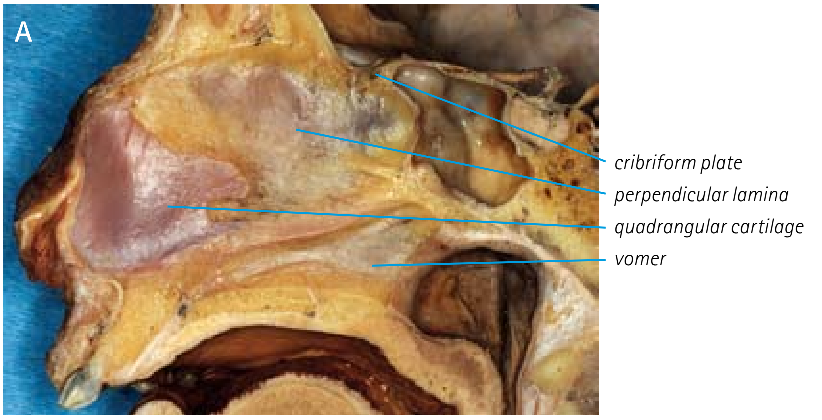


**Fig. 10** *The bony lateral wall of the nasal cavity (right side). The anterior portion is created by the compact frontal process of the maxilla and by the nasal bone (A). Similarly stable is the posterior part, formed by the maxillopalatine junction (B). The central part of the lateral wall, created by the inferior turbinate and ethmoid bone, is thin and fragile (C).*

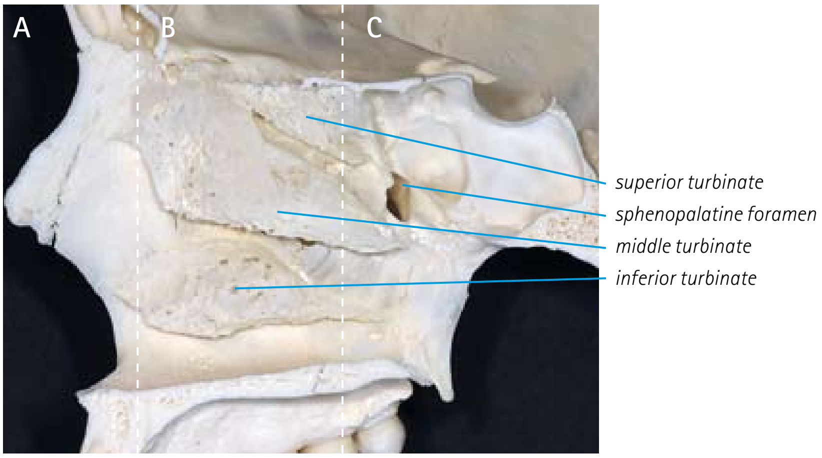

The central part of the lateral wall is thin and fragile. The most important anatomical landmarks for endoscopic orientation are located here, namely the turbinates and the spaces lying below them: the upper, middle and lower nasal meati (Figs. 8 A, 8 B, 10).

In front of the anterior wall of the sphenoid sinus is the superior turbinate. Here, medial from the superior turbinate, the sphenoid aperture (the natural opening of the sphenoid sinus) appears. In several cases, the aperture is covered by bony structures or by the nasal mucosa making identification complicated. The posterior ethmoidal cells enter under the superior concha into the superior meatus which is bordered anteriorly by the superior and middle conchae and posteriorly by the sphenoethmoidal recess (Figs. 11, 12).

Under the superior meatus is the middle concha. The middle turbinate is usually larger than the superior one. Its head is juxtaposed to the frontal process of the maxilla and it descends backwards in an oblique route whereas its tail is tangent to the inferior edge of the sphenopalatine foramen. A characteristic prominence can be seen at the point where the head of the turbinate is inserted corresponding to the region of the agger nasi (Figs. 11, 12).

The highly variable middle meatus can be exposed under the middle turbinate with the uncinate process in its anterior part. Originating at the agger nasi, the uncinate process ends imperceptibly near the body of the inferior turbinate. This area, covered mostly by a thin mucosal membrane, is the most fragile part of the lateral nasal cavity. Above the uncinate process is a regular, curved, and superiorly concave area, the semilunar hiatus. Above the semilunar gap, the ethmoidal bulla can be seen although exhibiting a highly variable anatomy (Fig. 12).

The inferior turbinate is voluminous and regular in shape showing a large anterior head followed by a long body that converges to form a thin tail (Fig.12). Below the anterior one third of the turbinate, the funnel-like nasolacrimal duct opens into the inferior meatus (Fig. 13). Dissecting along the inferior border of the nasal cavity through the inferior meatus, one can pass the posterior exit of the nasal cavity: the choana. The important landmarks of the epipharynx can be observed here, namely the torus tubarius and the tuba auditiva (Figs. 11, 13).

**Fig. 11** *The lateral wall of the left nasal cavity in a fixed specimen with the characteristic nasal turbinates. Note the main anatomical connections of the nasal cavity demonstrated by coloured wires (red wire: sphenoid aperture; yellow and blue wires: posterior ethmoidal cells; white wire: maxillar sinus; green wire: nasolacrimal duct; orange wire: tuba auditiva).*

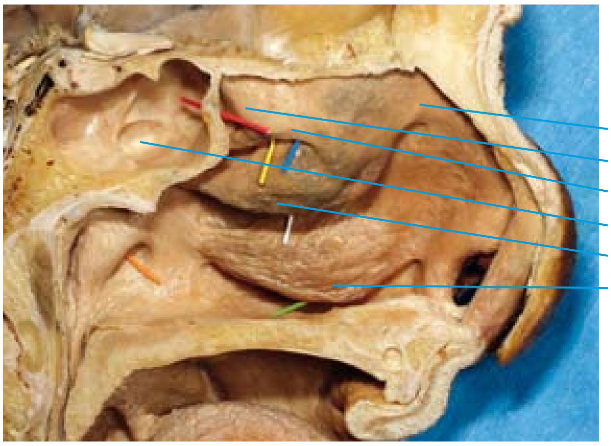


**Fig. 12** *Observation of the superior and middle meatus after resection of the superior and middle turbinates. Note the posterior ethmoidal cells, agger nasi, and the semilunar hiatus between the ethmoid bulla and uncinate process. The inferior turbinate is voluminous and regular in shape showing a large anterior head followed by a long body that converges to form a thin tail.*

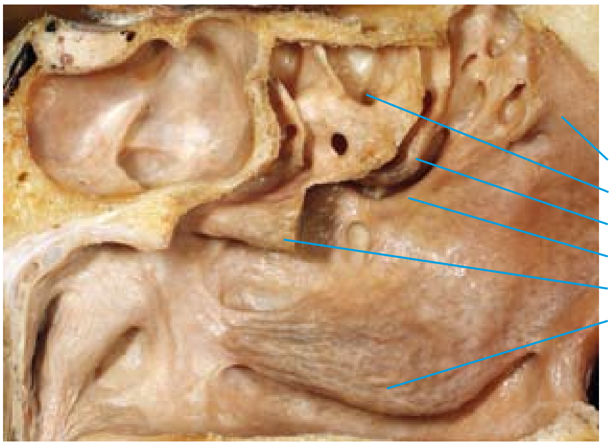


**Fig. 13** *The nasolacrimal duct entering into the infertior meatus is demonstrated with a green wire after partial resection of the inferior turbinate. Note the important landmarks of the epipharynx, e.g. the torus tubarius and the tuba auditiva (orange wire).*

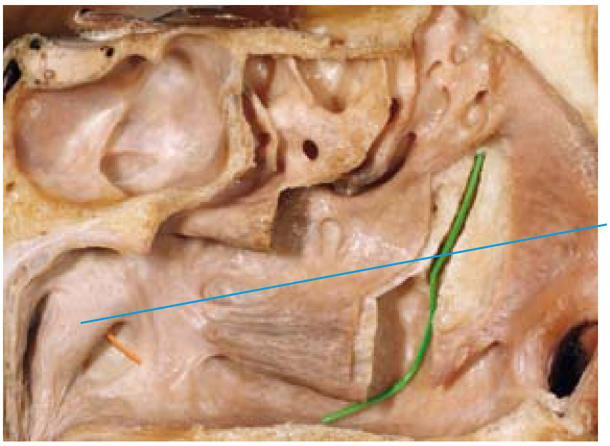

The neurovascular supply of the nasal cavity plays an important role when discussing the transsphenoidal exposure of the sphenoid sinus and sellar region. Basically, the nasal cavity is supplied by the maxillary artery and nerve, which arise from the external carotid artery and trigeminal nerve, complemented by branches of the ophthalmic artery and nerve deriving from the internal carotid artery and trigeminal nerve, respectively. Of particular importance are the olfactory filaments supplying the mucosal covering of the superior conchae, superior meati and the sphenoethmoidal recess on both sides.

The maxillary artery shows a short lateromedial course within the pterygopalatine fossa giving rise to small branches extending to the round and palatine canals and to the orbit. Still inside the fossa, a few millimetres from the sphenopalatine foramen and thus outside the nasal cavity, the maxillary artery divides into two terminal branches, the septal artery and the posterior lateral nasal artery. Some publications describe these two branches as a common vessel, called the sphenopalatine artery.

The septal artery passes the superior edge of the sphenopalatine foramen, ascending medially towards the anteroinferior part of the anterior wall of the sphenoidal sinus (Fig.14). When performing a direct endonasal endoscopic approach to the sellar region, this course becomes extremely important: drilling of the anterior wall can damage the artery causing arterial bleeding; however, this bleeding should not be confused with fatal damage to the internal carotid artery! At the nasal septum, the septal artery branches into the descending nasopalatine artery and several small calibre ascending branches.

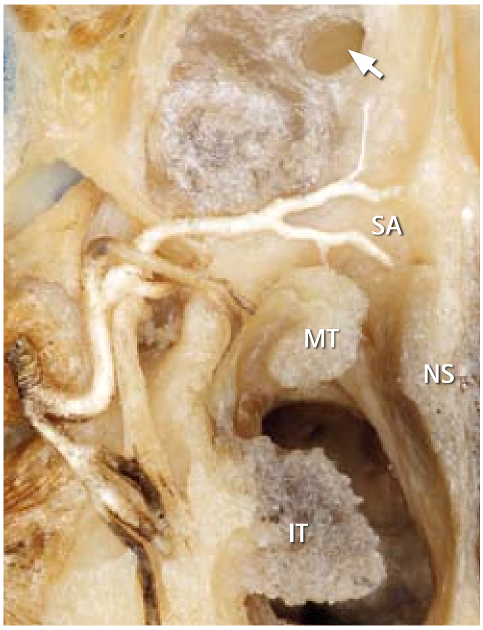


**Fig. 14** *Observation of the right septal artery from an anterior view. The vessel passes the sphenopalatine foramen and ascends medially towards the lower part of the anterior wall of the sphenoid sinus. The bony anterior wall of the sphenoid sinus is partially removed allowing observation of the intact sphenoid mucosa; note the sphenoid aperture (arrow). Caution is advised when performing a direct endonasal endoscopic approach to the sphenoid sinus: when drilling the anterior wall, the septal artery can be damaged causing disturbing arterial bleeding.*

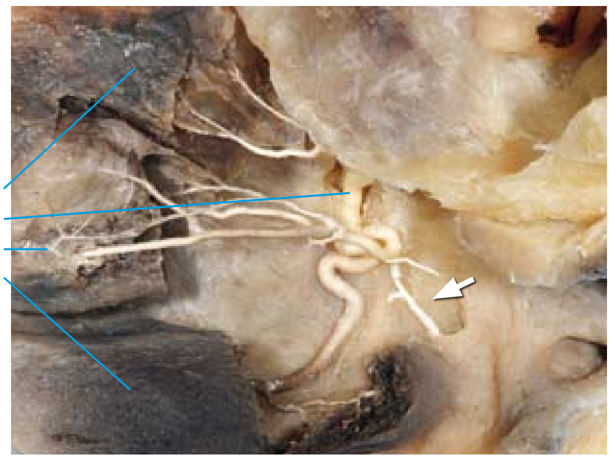


**Fig. 15** *The posterior lateral nasal artery crosses the sphenopalatine foramen and descends along the lateral wall of the nasal cavity (right side). Main branches supply the middle and inferior turbinates, some small ascending vessels run to the superior concha, building anastomoses with the posterior ethmoidal arteries. Note the posterior branches supplying the choanal region (arrow).*

The posterior lateral nasal artery crosses the inferior edge of the spheno-palatine foramen and descends along the lateral wall of the nasal cavity (Fig. 15). Main branches supply the middle and inferior turbinates. Some small ascending vessels run to the superior concha, building anastomoses with the posterior ethmoidal arteries. Posterior branches supply the choanal region.

## Sphenoid sinus

Located in the sphenoid body, the sphenoid sinus is the most posterior paranasal cavity communicating with the sphenoethmoid recess through the sphenoid apertures (Fig. 11). Around the sphenoid sinus there are a number of essential anatomic structures which usually extend into the cavity through the bony wall (Fig. 16). It is important to note that these structures

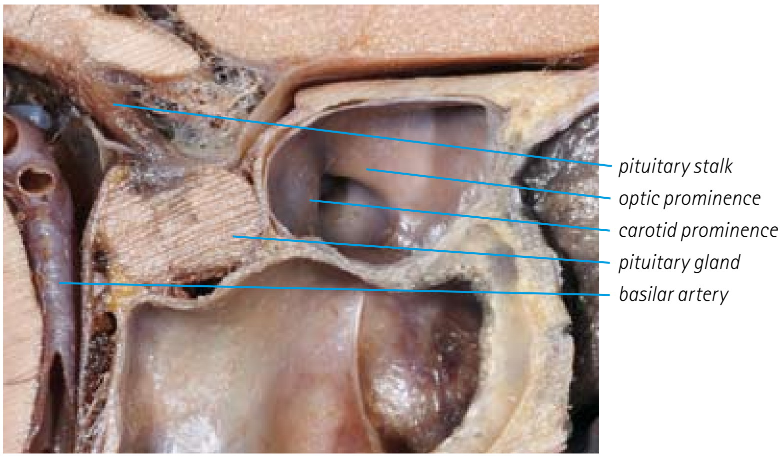


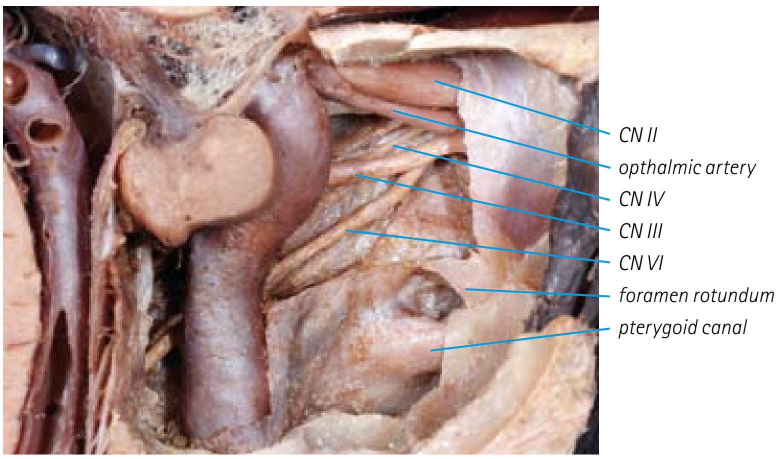


**Fig. 16** *The sphenoid sinus in a paramedian sagittal section of a fixed specimen. Note the characteristic prominences of the lateral sinus wall. After removal of the lateral sinus wall, neurovascular structures of the left cavernous sinus becomes visible.*

are not variable at all. It is only their appearance which changes individually according to the degree of pneumatization! The optic nerve runs in the bony optic canal at the craniolateral end of the cavity. Below and behind the optic nerve, the S-shaped form of the carotid canal and prominence of the mandibular branch of the trigeminal nerve at the foramen rotundum can be seen. At the bottom of the cavity, the pterygoid canal consisting of the major and deep petrous nerves bulges inwards and finally in the mediansaggital plane at the posteriosuperior end of the sinus, the prominence of the sella turcica can be seen (Fig. 17).

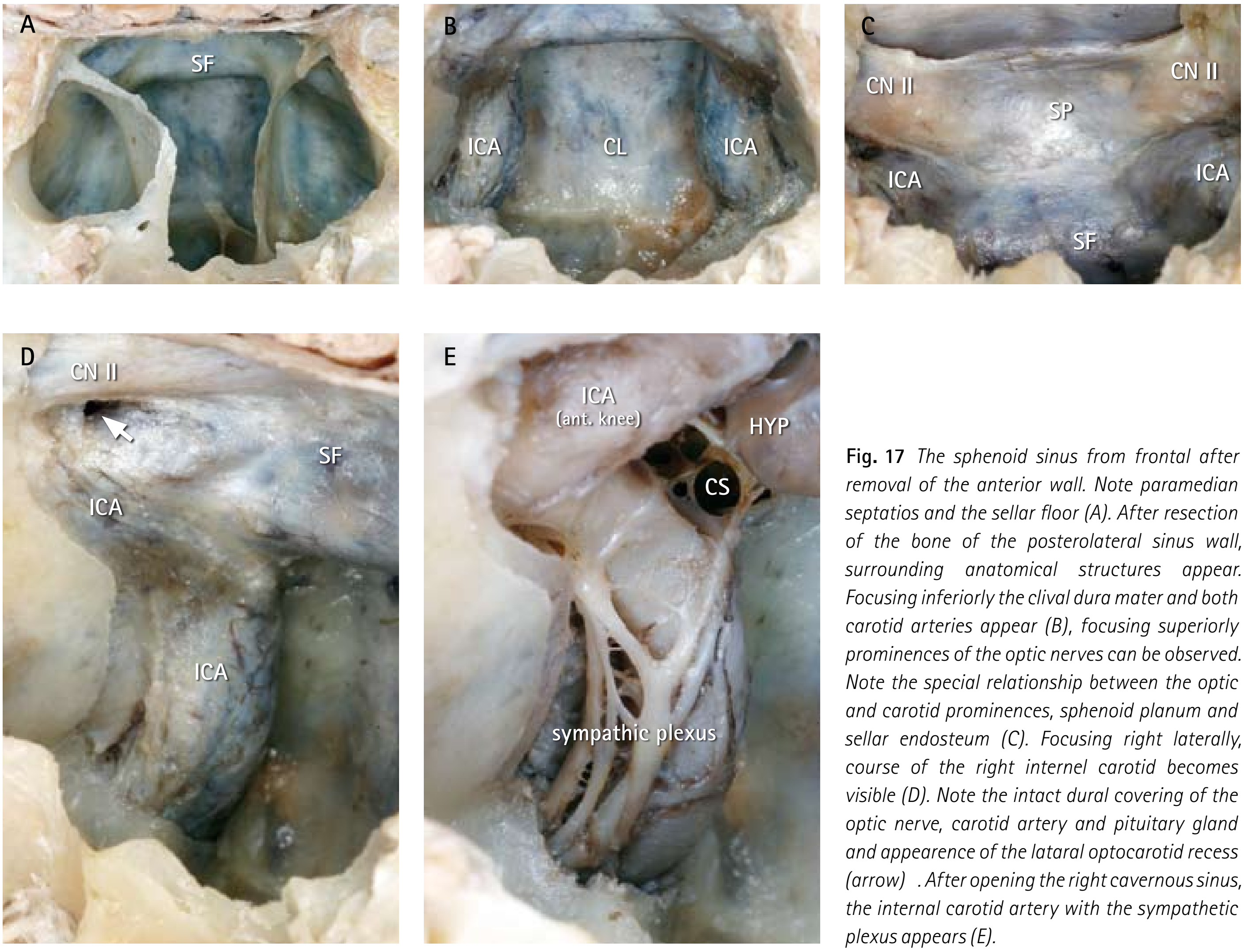


**Fig. 17** *The sphenoid sinus from frontal after removal of the anterior wall. Note paramedian septatios and the sellar floor (A). After resection of the bone of the posterolateral sinus wall, surrounding anatomical structures appear. Focusing inferiorly the clival dura mater and both carotid arteries appear (B), focusing superiorly prominences of the optic nerves can be observed. Note the special relationship between the optic and carotid prominences, sphenoid planum and sellar endosteum (C). Focusing right laterally, course of the right internel carotid becomes visible (D). Note the intact dural covering of the optic nerve, carotid artery and pituitary gland and appearence of the lataral optocarotid recess (arrow) . After opening the right cavernous sinus, the internal carotid artery with the sympathetic plexus appears (E).*

**The supra- and parasellar regions**

To work within the supra- and parasellar areas in a three dimensional plane, it is best explained in a geometric way as a virtual pyramid (Fig. 18). Each of the triangular planes of the sellar pyramid is defined by certain structures. The anterior plane of the pyramid is formed almost completely by the optic nerves, chiasm and the lamina terminalis. The first segments of the anterior cerebral arteries and the anterior communicating artery are also in direct relationship to this plane. The side of the pyramid includes the optic nerve and tract, the oculomotor nerve, the internal carotid artery and its two supraclinoid branches, and the posterior communicating and arterior choroidal arteries. The posterior pyramidal plane is defined by the ventral surface of the brainstem and basilar artery with the posterior cerebral and superior cerebellar arteries. The axis of the pyramid is formed by the infundibulum and pituitary stalk. The base of the pyramid corresponds to the sella turcica with the bilateral caverous sinus.

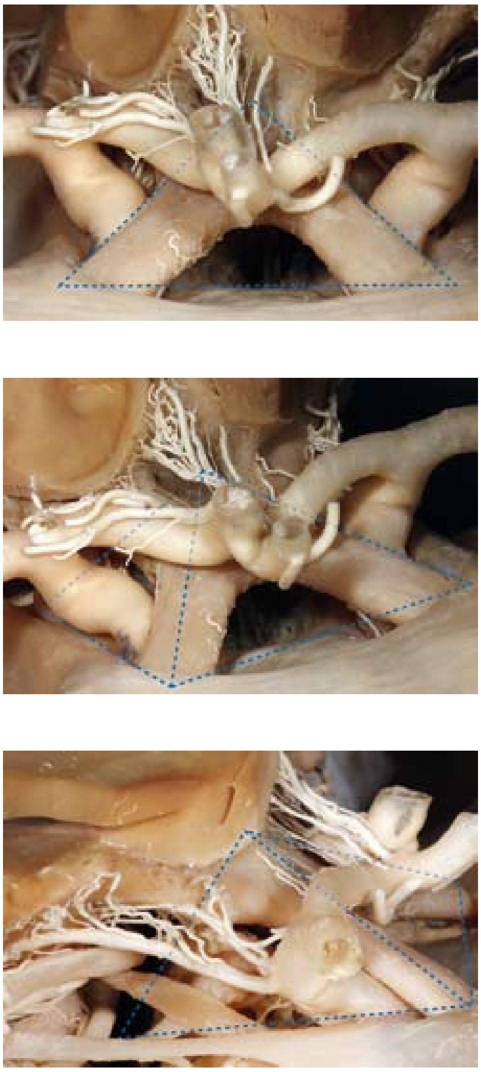

**Fig. 18** *The suprasellar region can be best explained in a geometric way as a virtual pyramid. Each of the triangular planes of the sellar pyramid is defined by certain neurovascular structures, observed from anterior (A), anterolateral (B) and lateral direction (C). Note small perforators supplying the lamina terminalis and the optic tract.*

From a surgical point of view, the cavernous sinus can be divided into three major anatomical parts (Fig. 19). The anterior part is particularly important when dealing with a transsphenoidal exposure. The dura mater covering the inferior surface of the anterior clinoid process and the proximal dural ring of the internal carotid artery form the roof of this anterior part of the cavernous sinus. Just underneath this dural layer are the oculomotor, trochlear and ophthalmic nerves coursing towards the superior orbital fissure. The middle part of the cavernous sinus represents the real venous chamber with structures of the lateral sinus wall consisting of the oculomotor, trochlear and ophthalmic nerves and the underlying horizontal segment of the carotid artery with the abducent nerve. The posterior part involves the region of the petrous bone tip including the Dorello's canal with the abducent nerve, the posterior knee of the carotid artery and the Gasserian ganglion.

The branching pattern of the internal carotid artery and arterial supply of the pituitary gland is of special surgical interest. The most prominent intracavernous branch, the meningohypophyseal trunk takes its origin from the internal carotid artery in the posterior part of the cavernous sinus, and divides into three groups of smaller branches, the tentorial, clival and sellar branches. The sellar branches, also termed inferior hypophyseal arteries, supply the pituitary gland and build an important anastomosis with the supraclinoidal branches of the internal carotid artery (Fig. 20). These thin branches, also called superior hypophyseal arteries supply the stalk and upper pituitary gland.

**Fig. 19 A** *Fixed specimen showing the neurovascular structures of the right cavenous sinus after removal of the lateral and upper sinus wall. The oculomotor, trochlear and ophthalmic nerves are retracted; note the intracavernous segment of the abducent nerve running on the internal carotid after passing the Dorello's canal below the Gruber's ligament. From a surgical point of view, the cavernous sinus can be divided into three major anatomical portions: the posterior (a), middle (b) and anterior (c) parts. The anterior part is particularly important for a transsphenoidal exposure.*

**Fig. 19 B** *Paraclinoid segment of the left internal carotid artery after removal of the anterior clinoid process. Note the paraclinoid carotid segment between the proximal (*) and distal (**) dural rings. The arrow points on the origin of the opthalmic artery.*

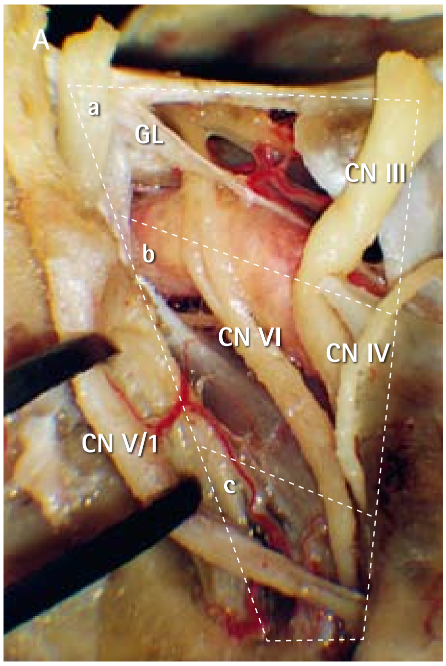


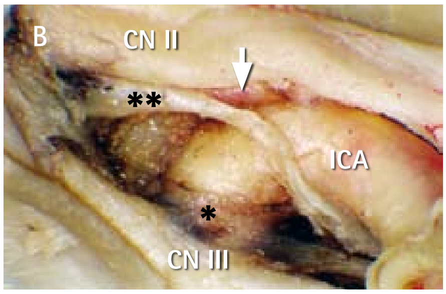


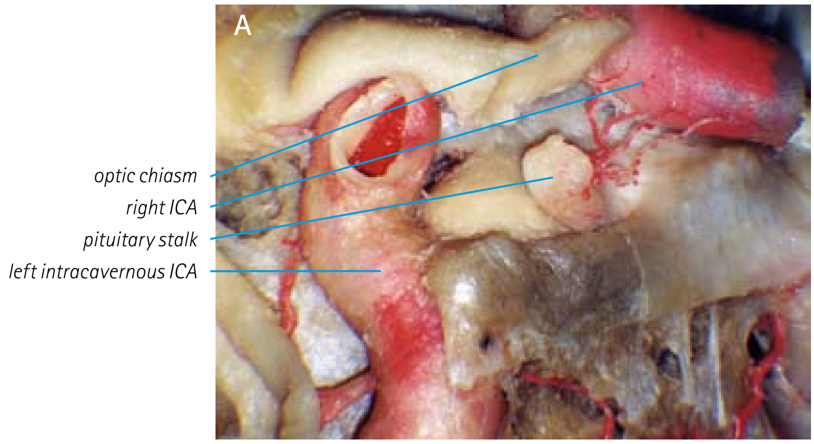


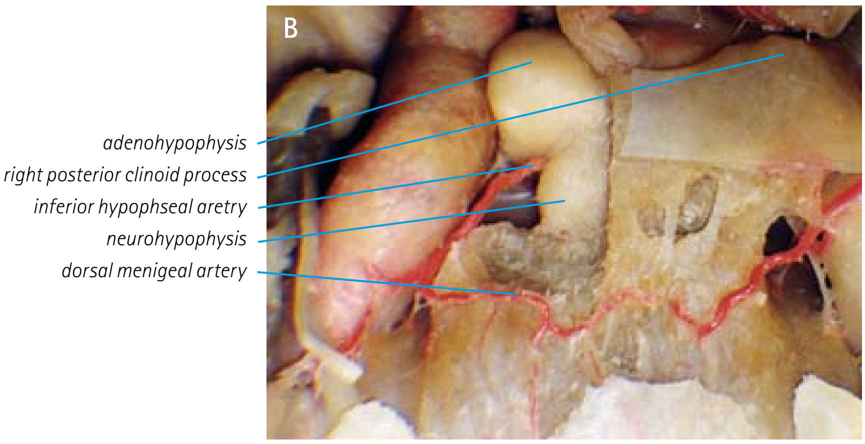


**Fig. 20 A, B** *Arterial supply of the pituitary gland. Note the superior hypophyseal branches, originating from the supraclinoid carotid artery (A). After removal of the left posterior clinoid process the inferior hypophyseal and dorsal meningeal arteries can be observed (B). Note the adeno- and neurohypophysis.*

# Endoscopic anatomy of the nasal cavity and sellar region

In the following the most important anatomical landmarks of the nasal cavity and the para- suprasellar area are demonstrated in a fresh human cadaver using a 4 mm endoscope with a 30° viewing angle (Figs. 21 – 51).

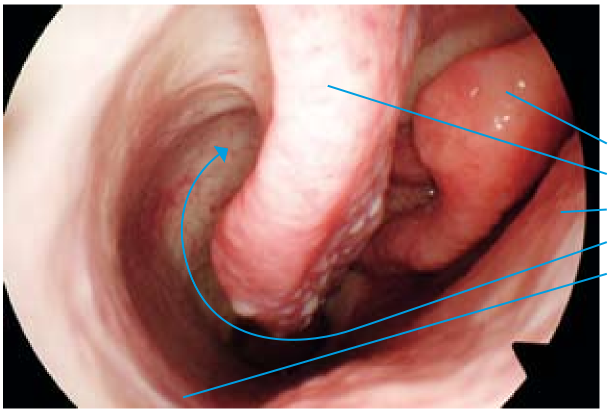


**Fig. 21** *Overview of the nasal cavity. The tip of the endoscope is placed into the right nostril. Note the floor and medial wall of the cavity. The inferior turbinate and inferior meatus are clearly apparent.*

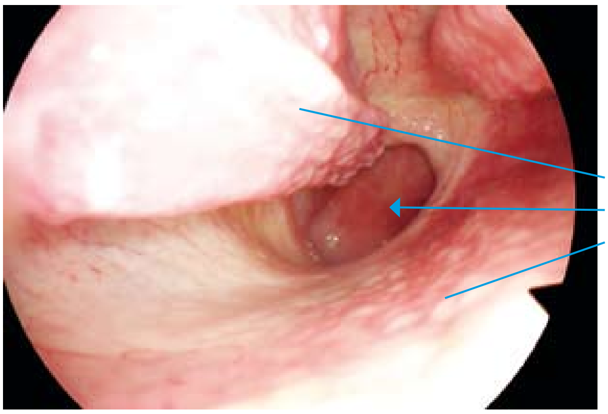


**Fig. 22** *The endoscope is introduced along the inferior turbinate approaching the choanal region. Note the posterior tail of the inferior turbinate.*

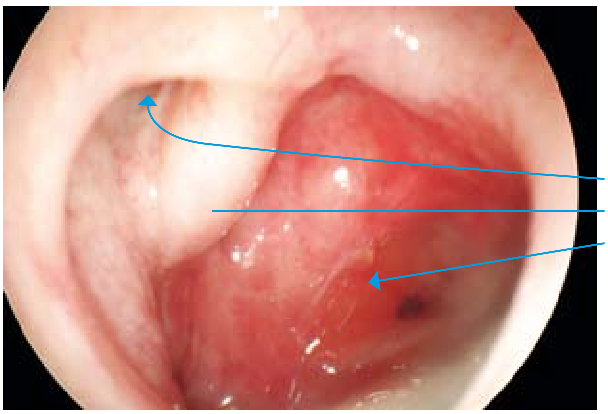


**Fig. 23** *Approaching the epipharynx, the 30° endoscope is rotated to the right with visualization of the entrance of the tuba auditiva. Note the torus tubarius and the posterior wall of the pharynx.*

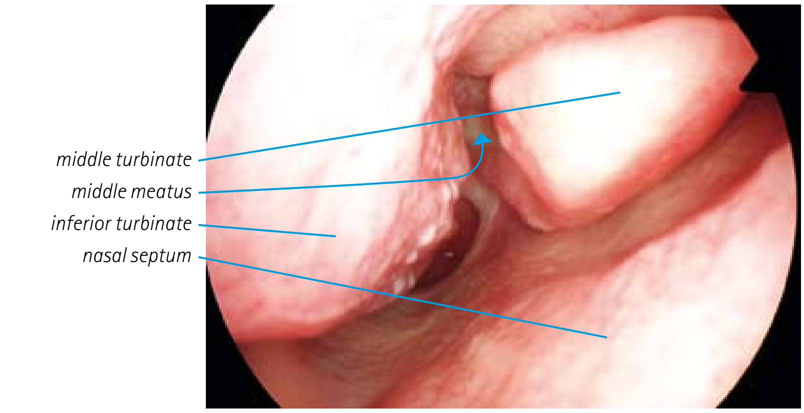


**Fig. 24** *Retracting the endoscope, the head of the middle turbinate is exposed. Note the path into the middle meatus.*

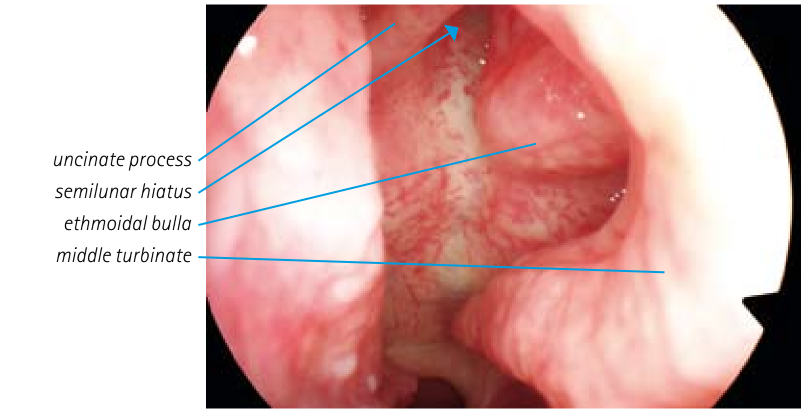


**Fig. 25** *Using a 30° endoscope, the middle meatus is observed. Note the junction of the uncinate process with the ethmoidal process of the inferior turbinate. The semilunar hiatus appears between the uncinate process and the ethmoidal bulla connecting the maxillar sinus with the nasal cavity.*

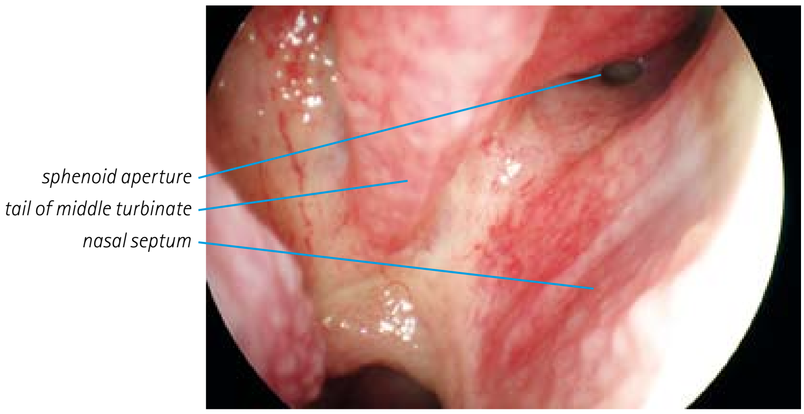


**Fig. 26** *Following the inferior border of the middle turbinate, its insertion into the pterygoid bone is approached. Note the lower part of the anterior wall of the sphenoid sinus and the sphenoid aperture.*

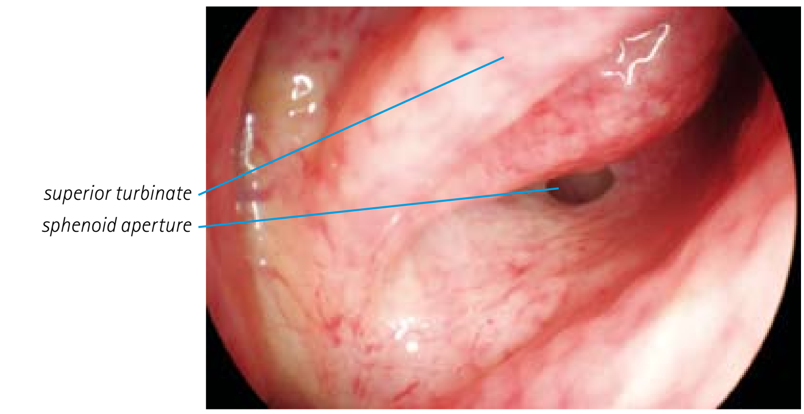


**Fig. 27** *Moving upwards, the endoscope reaches the sphenoethmoidal recess. Note the superior turbinate and the entrance to the sphenoid sinus.*

**Fig. 28** *The superior turbinate is moved to medial exposing the superior meatus. Note the view into the posterior ethmoidal cells.*

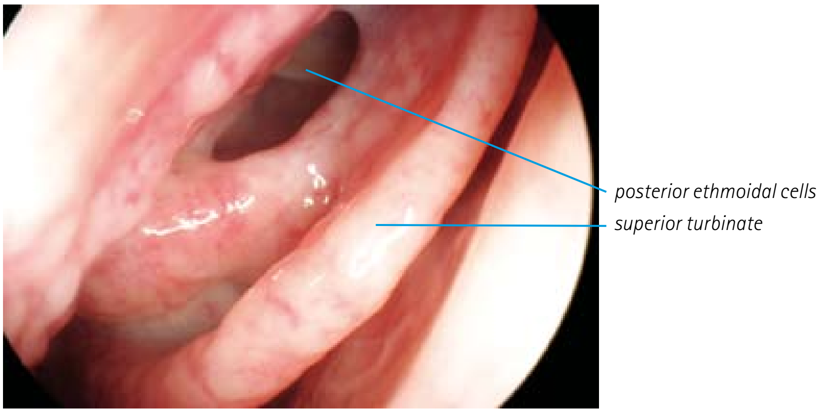


**Fig. 29** *Opening the anterior wall of the sphenoid sinus with a diamond drill. Typical placement of drilling is medial from the superior turbinate just inferiorly from the sphenoidal aperture and ca. 1 cm over the choana.*

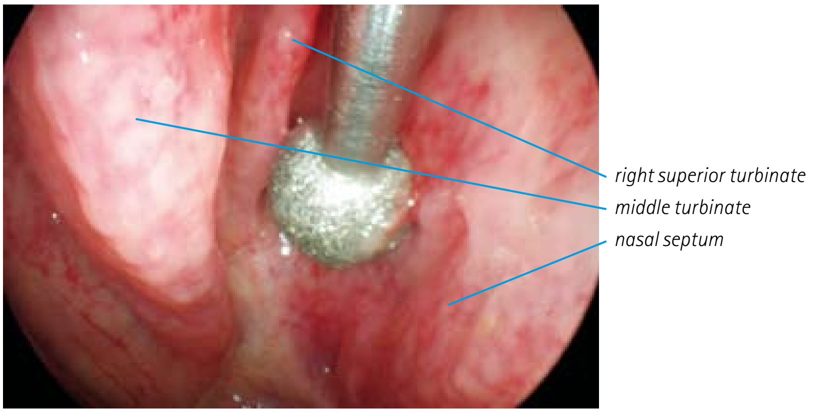


**Fig. 30** *After drilling, the view into the sphenoid sinus becomes clear. Note the left paramedian septum with intact mucosa on the left side. On the right side, we gain a superb overview of the anatomical structures with direct visualization of the optic and carotid prominences, the lateral optocarotid recess and the sellar floor.*

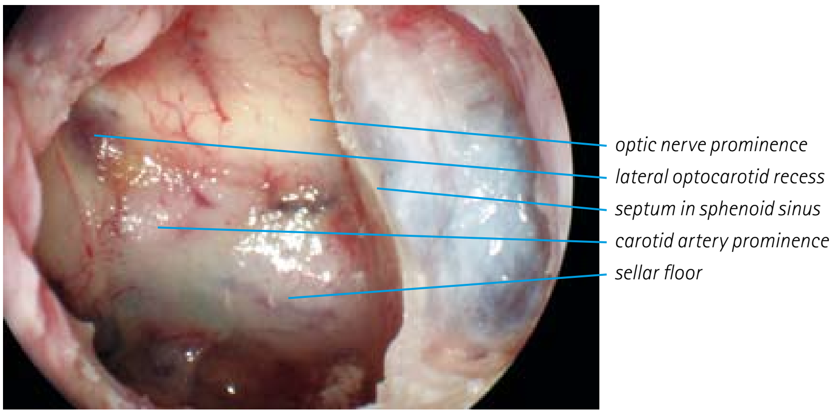


**Fig. 31** *After completing the unilateral exposure, the approach is continued on the contralateral side in a similar manner allowing biportal binostril dissection within the deep-seated surgical field. Note the drill medial from the left superior turbinate.*

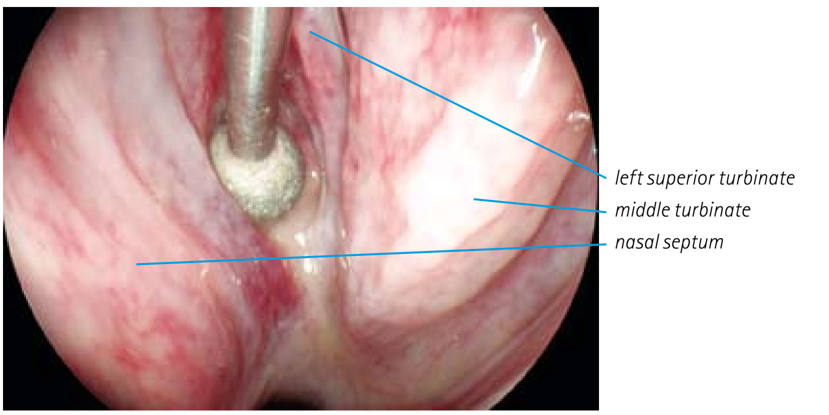

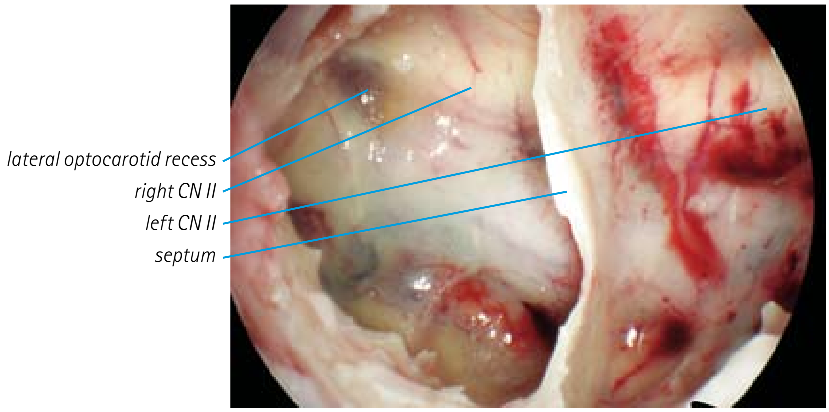


**Fig. 32** *View into the sphenoid sinus from the left nostril before removal of the sphenoid septum. Note the impression of the both optic nerves and the right lateral optocarotid recess.*

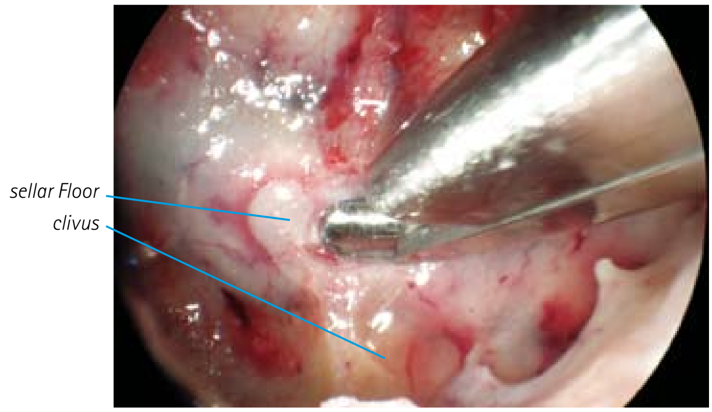


**Fig. 33** *The endoscope is placed through the right nostril, the Kerrison punch is introduced from the left to open the sellar floor. Note the perfect contra-lateral visualization without conflict between the endoscope and instrument.*

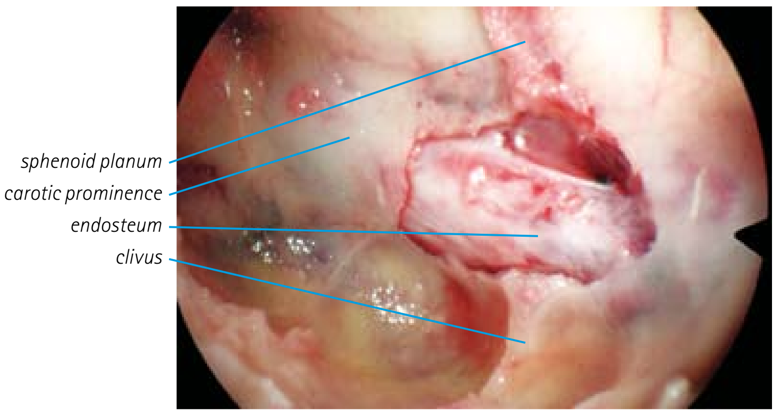


**Fig. 34** *Appearance of the sellar endosteum after removal of the bony sellar floor.*

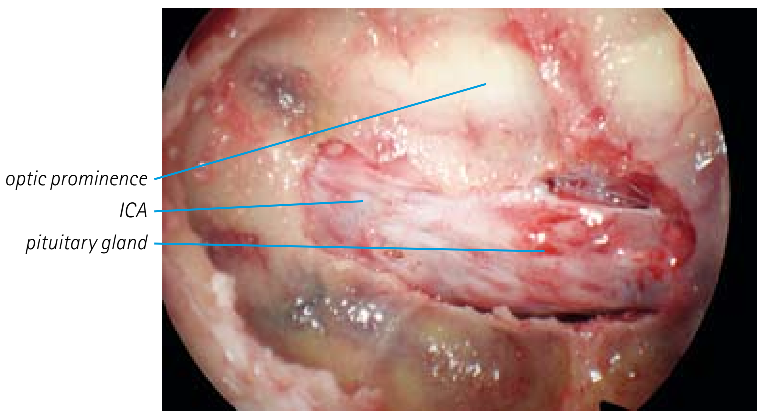


**Fig. 35** *After further bony resection, the anterior knee of the right internal carotid artery is exposed. Note the optic prominence.*

**Fig. 36** *The view of the 30° endoscope is directed frontally and the sphenoid planum is opened observing the dura mater of the anterior fossa.*

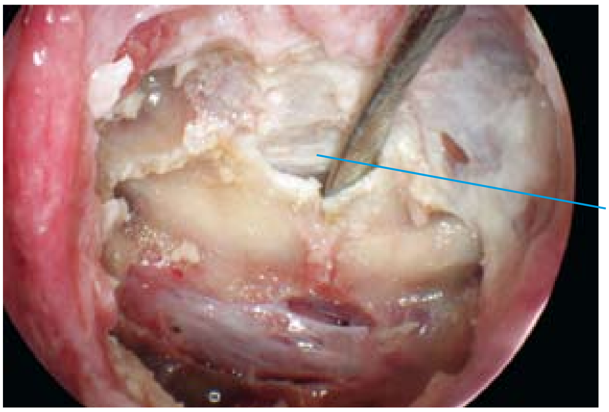


**Fig. 37** *After further dissection, the anterior fossa is entered. Note the right gyrus rectus, the olfactory and optic nerves. The proximal optic canal is opened. Note the distal dural ring indicating the border between the paraclinoid and supraclinoid carotid arteries.*

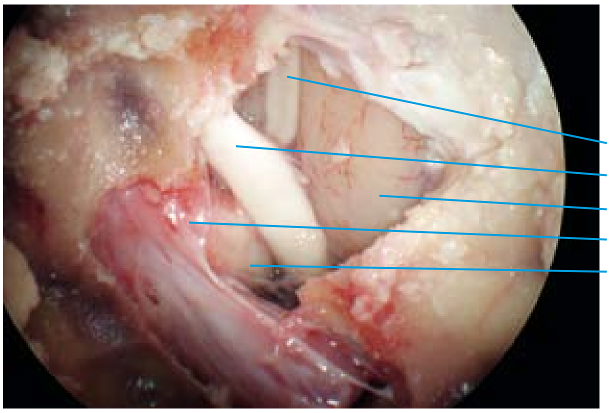


**Fig. 38** *With further removal of the planum, the chiasm and both optic nerves are exposed via the special transsphenoidal route.*

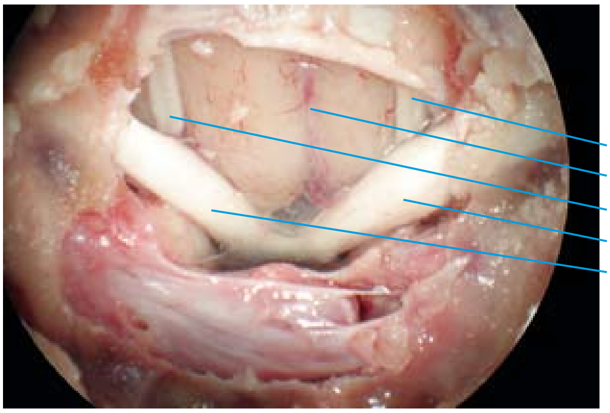


**Fig. 39** *The optic chiasm in a close-up position of the endoscope. In the background, the reddish pituitary stalk can be seen.*

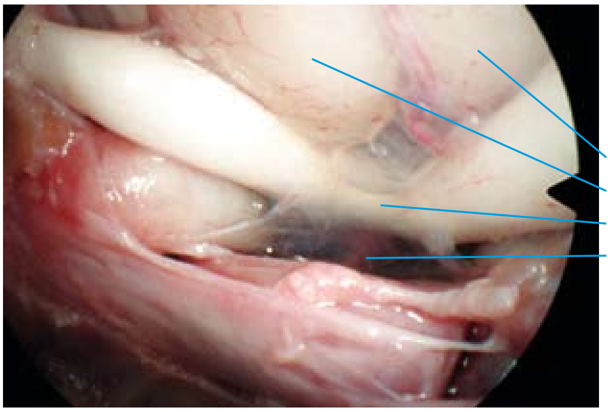

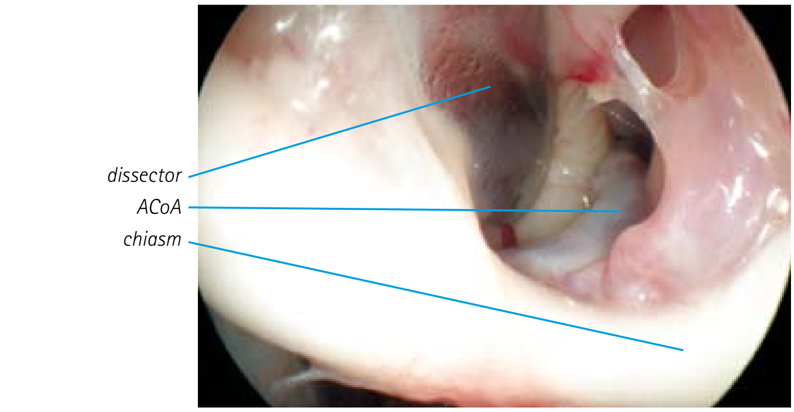


**Fig. 40** *After opening the lamina terminalis cistern, the anterior communicating artery complex is approached.*

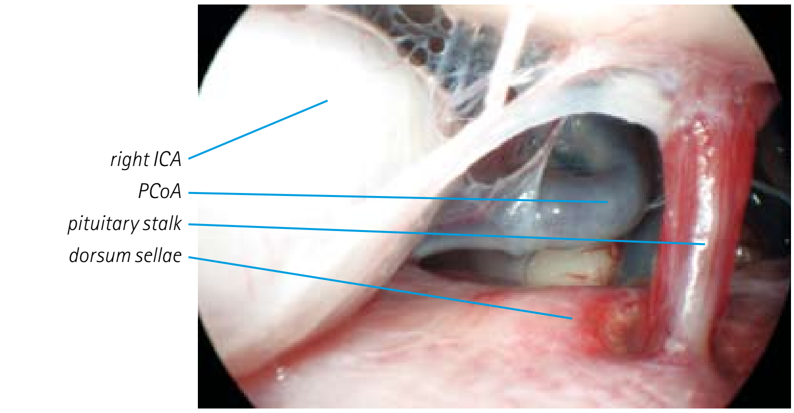


**Fig. 41** *The chiasma cistern is carefully opened. The deep-seated prepontine region appears through the anatomical window between the right internal carotid artery and the stalk. Note the dorsum sellae and the right posterior communicating artery in the background.*

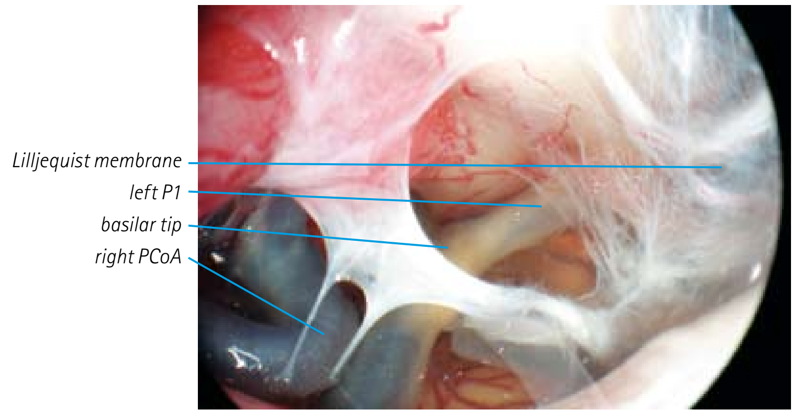


**Fig. 42** *The endoscope is introduced through the left stalk – carotid gap. Note the fine remnants of the Lilljequist membrane; the basilar tip appears in the background. The left P1 segment of the posterior cerebral artery and the prominent right posterior communicating artery become visible.*

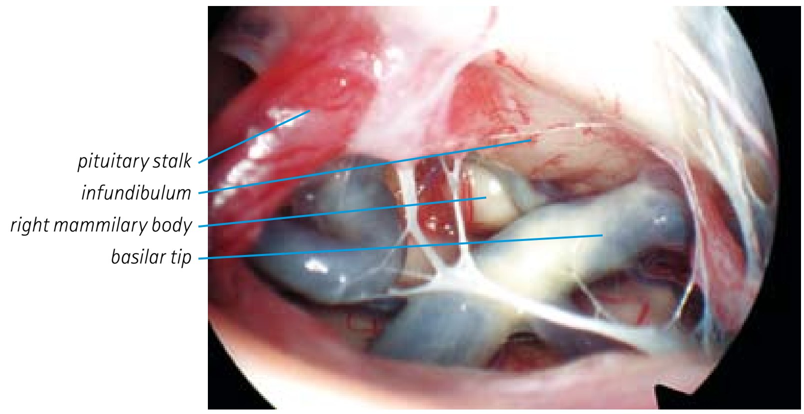


**Fig. 43** *Endoscopic visualization of the distal basilar artery. Note the infundibulum and pituitary stalk.*

**Fig. 44** *The basilar bifurcation in a close-up position. Note the hypoplastic P1 segment of the right posterior cerebral artery, right mammilary body, and the origin of the oculomotor nerve.*

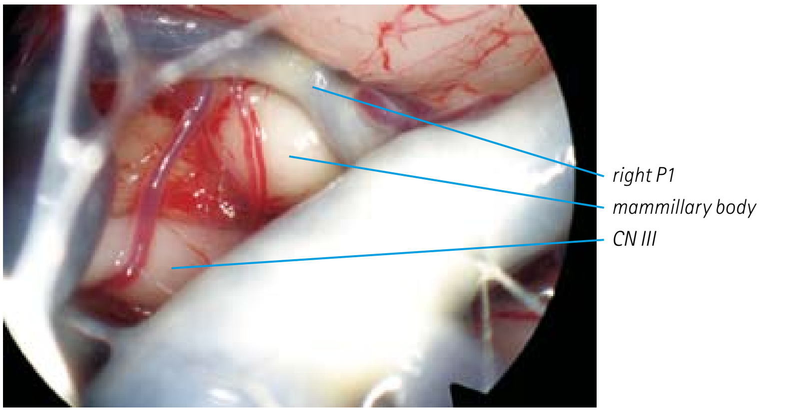


**Fig. 45** *The 30° endoscope is rotated to the right and the left posterior cerebral artery is followed in a lateral direction. Note the special relationship between the left posterior communicating artery, the P2 segment, the optic tract and the A1 segment of the left anterior cerebral artery.*

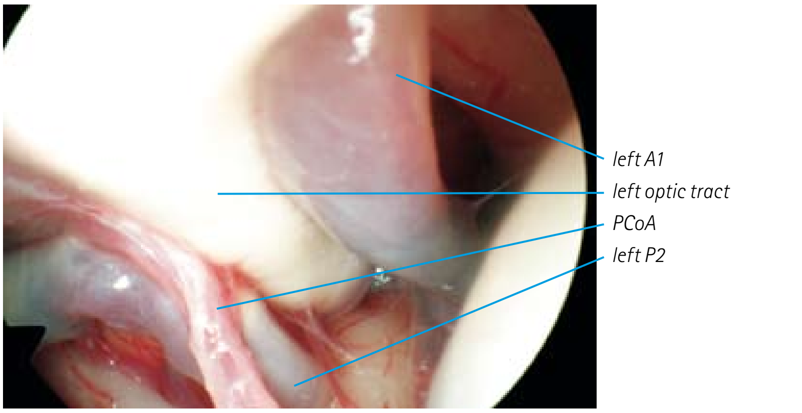


**Fig. 46** *Following the A1 segment, the left carotid bifurcation is reached.*

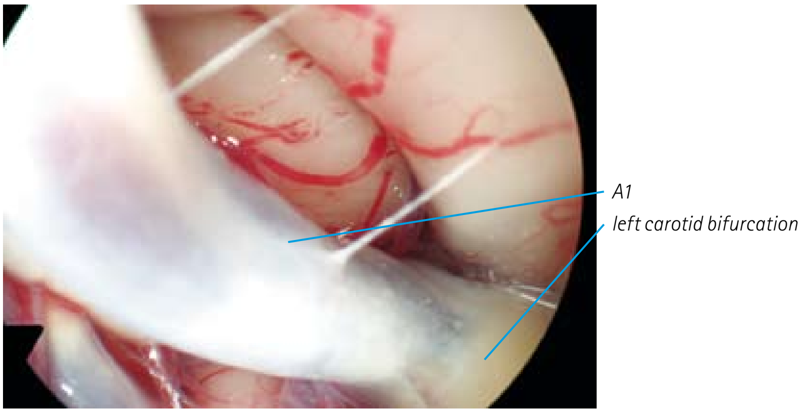


**Fig. 47** *Retracting the endoscope, the sphenoid sinus is again exposed. Using a fine drill, the clivus is drilled basal from the pituitary gland visualizing the dura mater of the posterior fossa. Note the proximal and distal dural rings indicating the paraclinoid carotid artery.*

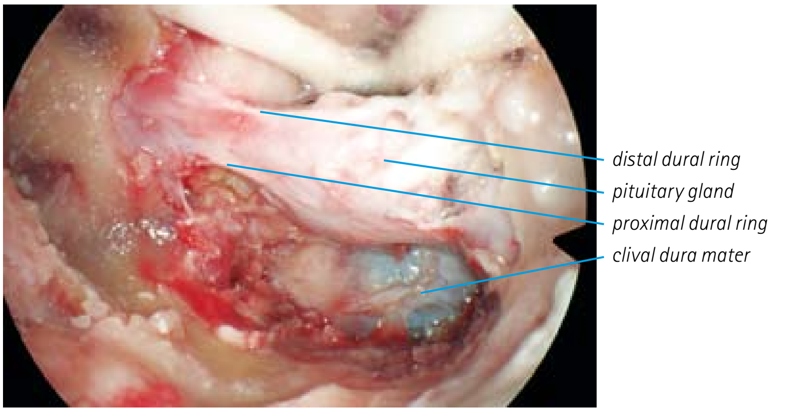

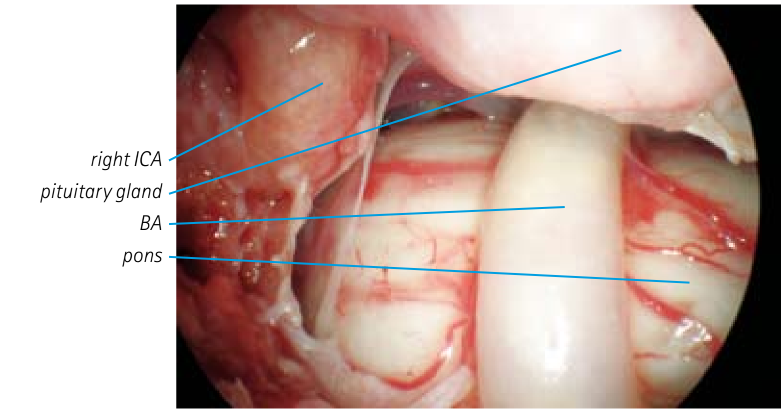


**Fig. 48** *After opening the clival dura, the prepontine cistern with the basilar artery appear. Note the relation between the posterior knee of the right intracavernous internal carotid and basilar arteries.*

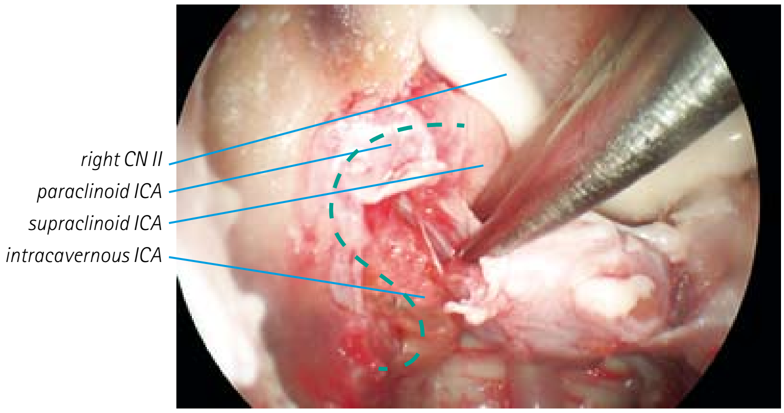


**Fig. 49** *The proximal and distal dural rings are divided with microscissors allowing mobilization of the pituitary gland. Note the S-formed course of the intracavernous – paraclinoid – supraclinoid carotid artery (dashed line).*

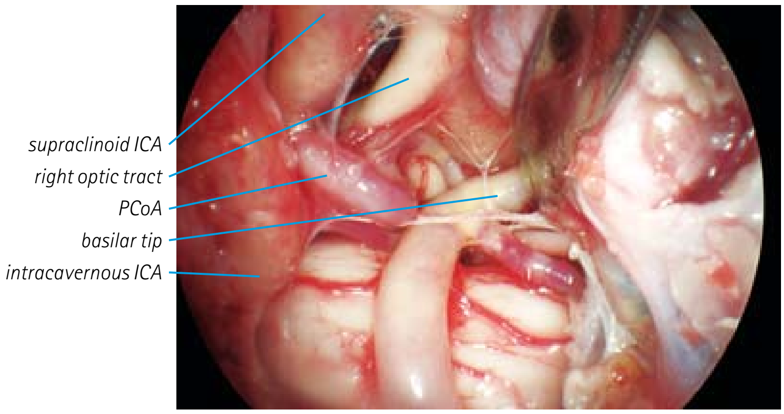


**Fig. 50** *The pituitary gland is retracted with a fine microdissector allowing endoscopic investigation of the prepontine and interpeduncular regions.*

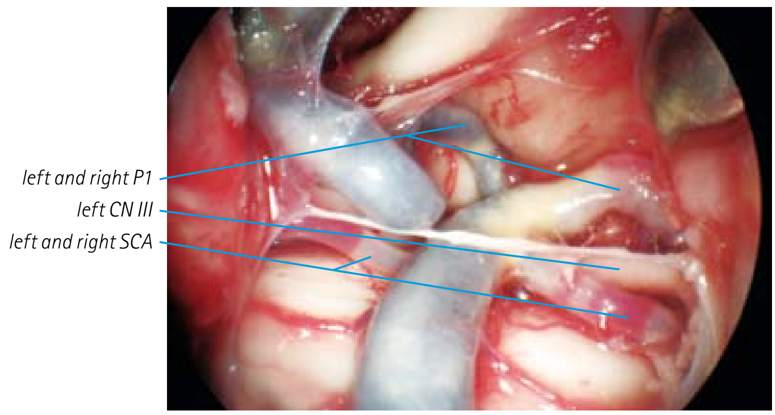


**Fig. 51** *Close-up investigation of the distal basilar artery. Note the left oculomotor nerve between the posterior cerebral and superior cerebellar arteries.*

# The endosnasal transsphenoidal biportal approach

Most publications on endoscopic transsphenoidal surgery describe a monoportal – mononostril exposure of the central skull base (Fig. 52 A). These mononostril approaches may cause only unilateral traumatization of the nasal cavity; however, they offer several disadvantages. Without using a nasal speculum, the space within the nasal cavity is very narrow causing subsequent limitation in surgical manipulation. The tip of the endoscope disturbs the introduction of instruments and because of the lack of space, the nasal mucosa can be severely damaged. To allow adequate dissection, a nasal speculum may be required or removal of the middle and superior turbinates may be necessary.

By comparison, the biportal approach offers free introduction and improved manoeuvrability of the surgical instruments because the endoscope is placed through the other nostril (Fig. 52 B). The tip of the endoscope does not disturb the surgical manipulation and the endoscope allows optimal contralateral visual control of tumor removal. The technique avoids the need for rhinoseptal submucosal dissection offering a direct and rapid approach to the sphenoid sinus. Without using a nasal speculum, surgical manipulation is not restricted with free manoeuvrability of instruments. The method avoids the need for postoperative nasal packing thus limiting breathing problems and discomfort after surgery.

**Fig. 52** *Using monoportal exposure, the space within the nasal cavity is very narrow causing subsequent limitation in surgical manipulation. The tip of the endoscope disturbs the introduction of instruments and because of the lack of space, the nasal mucosa can be severely damaged (A). By comparison, using a biportal approach the tip of the endoscope does not disturb the surgical manipulation and the endoscope allows optimal contralateral visual control of tumor removal. The free introduction and improved manoeuvrability of the surgical instruments can be achieved because the endoscope is placed through the other nostril (B).*

A

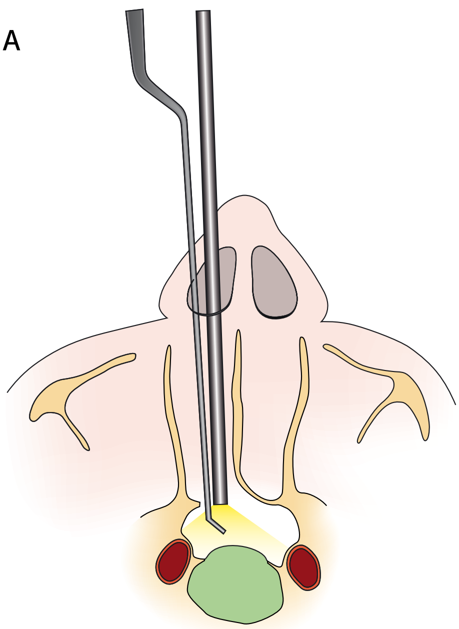

B

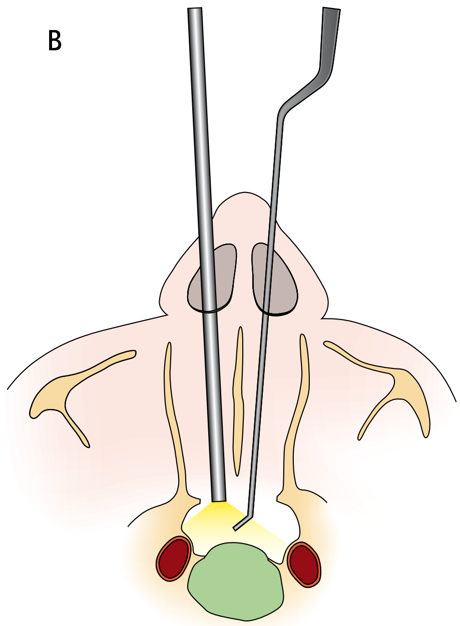

## Positioning and preparation of the patient

In the supine position, the head is elevated to avoid venous congestion of the parasellar sinusoid vessels. The head is rotated and slightly lateroflected allowing efficient dissection during the operation. The neurosurgeon remains beside the patient and has optimal control of the endoscopic and fluoroscopic or neuronavigation monitor (Fig. 53). After installation of the C-arm or neuronavigation, the midlle turbinates are lateralized with a nasal speculum and a nasal packing is introduced with mucosal disinfection and vasoconstrictor.

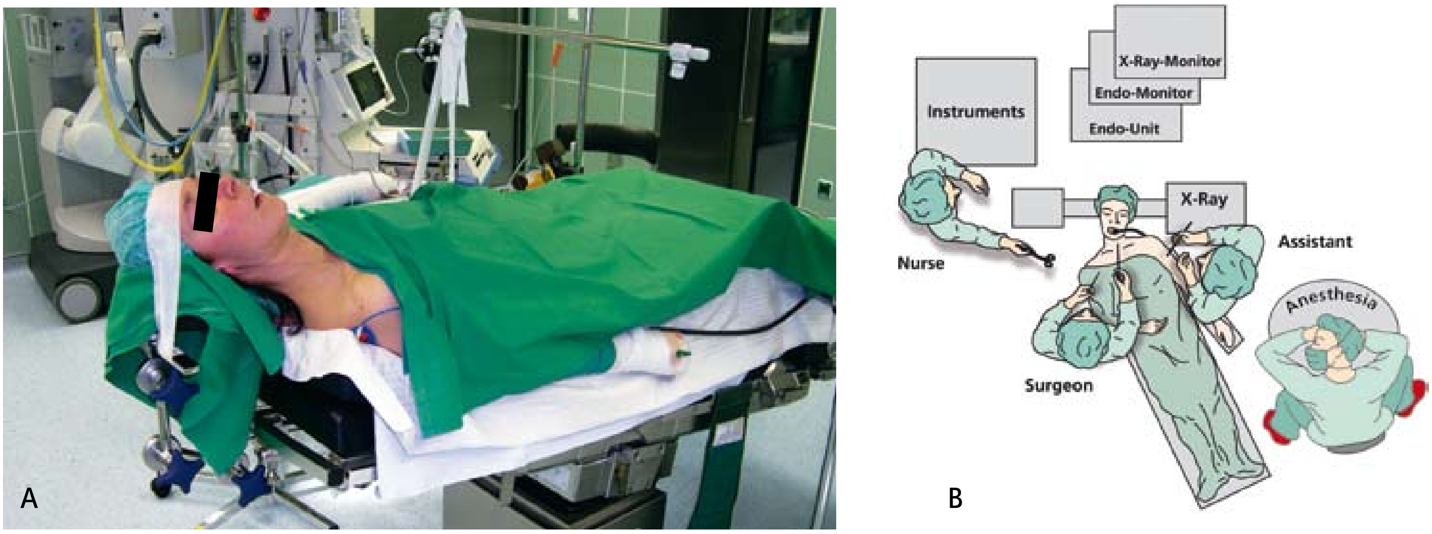


**Fig. 53** *The patient is placed supine, the head is rotated and slightly lateroflected allowing efficient dissection during the operation (A). The neurosurgeon remains beside the patient and has optimal control of the endoscopic and fluoroscopic or neuronavigation monitor. Schematic illustration demonstrating the lay-out of the operating theatre when performing endoscopic transsphenoidal surgery (B).*

# Steps of the biportal approach

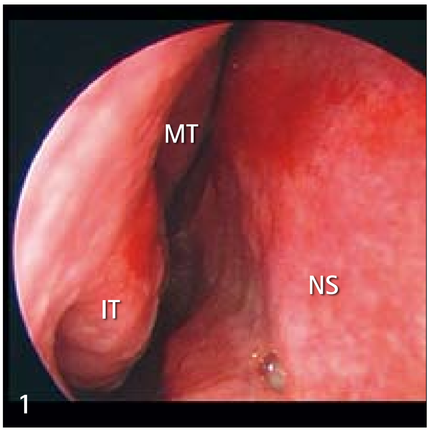


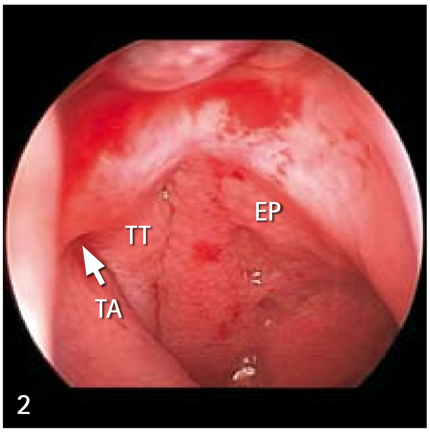


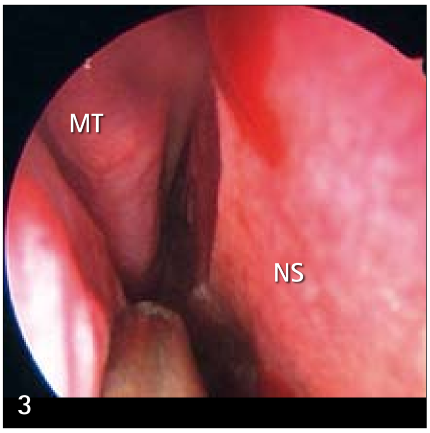


### Nasal step

After preparation of the patient, the endoscope is introduced into the nasal cavity. Important landmarks are identified on both sides: the first structure is the inferior turbinate. Along the inferior nasal meatus the choana is approached checking the epipharynx with the characteristic structures of the torus tubarius and tuba auditiva. Thereafter, the endoscope is moved upwards and the middle turbinate is recognized. After gentle lateralization of the middle turbinate, the endoscope is introduced along its anterior inferior border, exposing the sphenoethmoidal recess. Here, the superior turbinate is identified and pushed to the side exposing the sphenoid aperture. Medial and basal from the aperture, the mucosa is carefully coagulated avoiding bleeding from the septal artery and the anterior wall of the sphenoid sinus is opened with a diamond drill. Take care to avoid coagulation and damage to the superior turbinate and the upper sphenoethmoidal recess to prevent postoperative anosmia!

After unilateral exposition of the sphenoid sinus, the approach is completed on the contralateral side in a similar manner allowing biportal binostril dissection within the deep-seated surgical field (Figs. 54, 55)

**Fig. 54** *Intraoperative photographs showing the nasal part of the biportal approach.*
1. *The endoscope is introduced into the nostril visualizing the nasal cavity. Note the nasal septum, the inferior and middle turbinates.*
2. *Moving inferiorly, the upper part of the epipharinx is exposed through the choana. Note the torus tubarius and the tuba auditiva.*
3. *Dissecting upwards, the middle turbinate appears. In the background, the superior turbinate can be observed.*

### Sphenoid step

The septum of the sphenoid sinus can be removed with a diamond drill or grasping instruments should it be present and be a hindrance. The appearance of the anatomical landmarks depends on the pneumatization of the sphenoid bones; however, in most cases the sellar floor, clivus, sphenoid planum, optic nerves, carotid arteries and the optocarotid recess can be seen allowing a perfect anatomically based point of reference (Figs. 55, 56). A limited anatomical orientation can occur because of a conchal sella form, significant intra- and parasellar tumor extension and, especially, as a result of re-do surgeries. These cases are a particular surgical challenge where the use of intraoperative navigation is recommended.

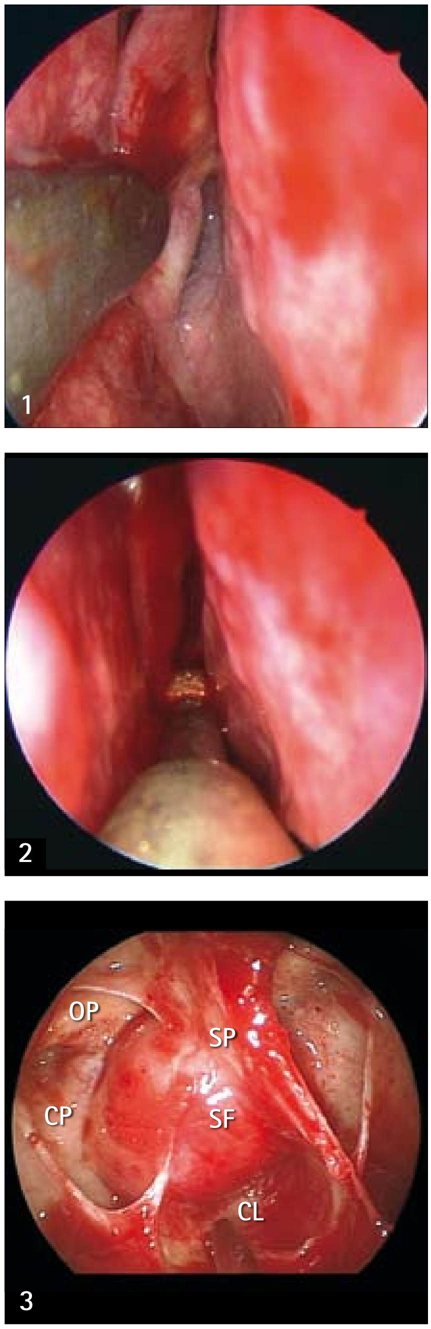


**Fig. 55** *Nasal and sphenoid steps of the biportal approach.*

1. *The superior turbinate is atraumaticaly lateralized allowing exposure of the sphenoethmoidal recess and the anterior wall of the sphenoid sinus.*
2. *After careful coagulation of the mucosa, the anterior wall is opened with a diamond drill.*
3. *View into the sphenoid sinus after completing the biportal approach. The anatomical structures of the central skull base, e.g. the sphenoid planum, optic prominence, carotid prominence and the clivus are well visualized. Note the tumorous enlarged sellar floor.*

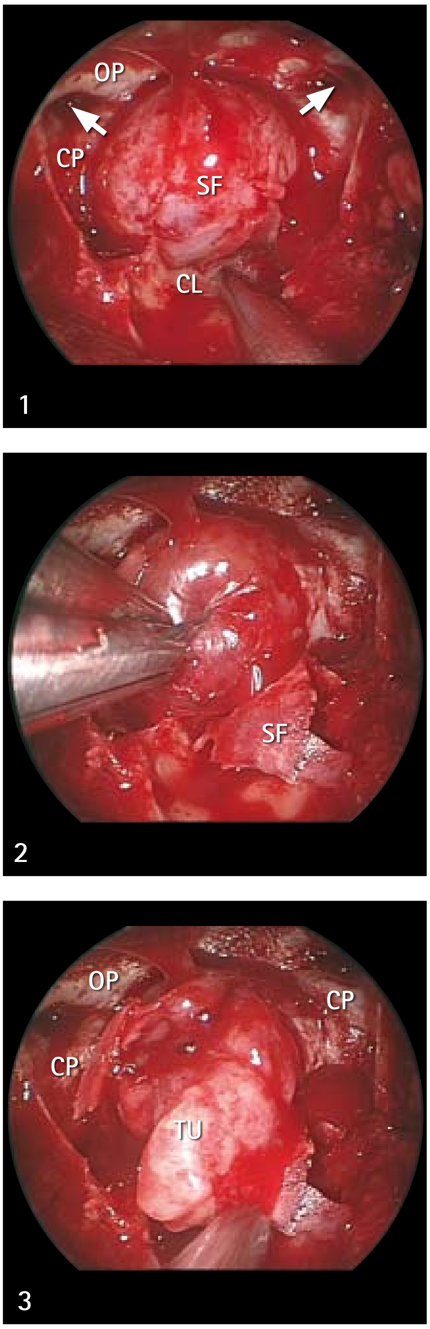


### Sellar step

Under secure visual control, the sellar floor is opened with a diamond drill and the opening enlarged with fine Kerrison punches. From this stage of surgery, the endoscope is fixed in the opposite nostril with a holding device and the dissection is continued in a bimanual manner. With the free nasal cavity, introduction and removal of instruments can be performed in an unhindered manner without the need for a nasal speculum. The dura is then opened with fine scissors or a microknife and the intrasellar lesion is removed with different curettes (Figs. 56 – 57). Principally, tumor resection should be started in the basal – clival part, then bilaterally. At least the suprasellar tumor tissue should be removed avoiding opening of the diaphragma sellae. If a CSF leak occurs, meticulous sheet-by-sheet closing is necessary.

### Para- and suprasellar step

The main advantage of the endoscopic technique is the direct visual investigation of hidden parts of the surgical field. Introducing the endoscope into the sellar chamber, suprasellar and intracavernous tumor remnants can by directly visualized and the complete removal can be monitored. In comparison with blind tactile control, the endoscopic surgeon is able to see pathoanatomical details which are always hidden for the microsurgical resection.

### Sellar reconstruction and closure

If no intraoperative CSF-leak occurs, special sellar reconstruction is unnecessary and therefore not recommended (Fig. 57). With minimal CSF loss, particular effort is not necessary and spongostane and fibrin glue can be used for effective closure. In the case of extensive leakage, the use of periumbilical abdominal fat tissue can be recommended. A specific surgical

**Fig. 56** *Sphenoid and sellar steps of the biportal approach.*

1. *After resection of sphenoid septations and partial removal of the sphenoid mucosa the tumorous enlarged sellar floor appears. Note the lateral optocarotid prominences on both sides (arrows).*
2. *The sellar endosteum is exposed and opened with fine microscissors. Note the secure optical control with direct visualization of the surrounding anatomical structures.*
3. *Using conventional instruments, the tumor is removed. According to the biportal way, there is no conflict between the instruments and the tip if the endoscope.*

challenge is, however, to close a wide dural gap, especially when performing extended approaches for removal of intradural lesions. For this reason, a sheet-by-sheet closing of the hiatus is essential; experienced neurosurgeons describe the use of a vascular nasoseptal or a time-consuming and complex temporoparietal fascial flap. Nevertheless, in these cases the cause of and reason for this extensive approach-related traumatization should be critically considered.

After leaving the sphenoid sinus, both nasal cavities are inspected and cleansed of coagulated blood. With the endonasal biportal technique without transseptal dissection, a nasal tamponade is not necessary and therefore not recommended.

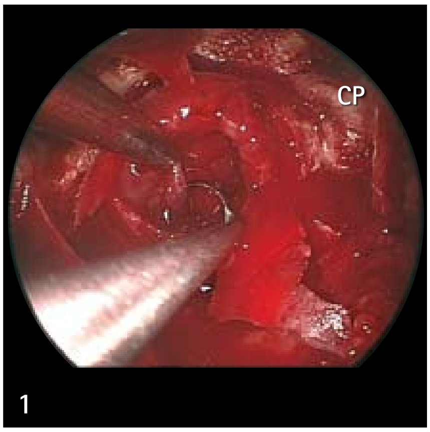


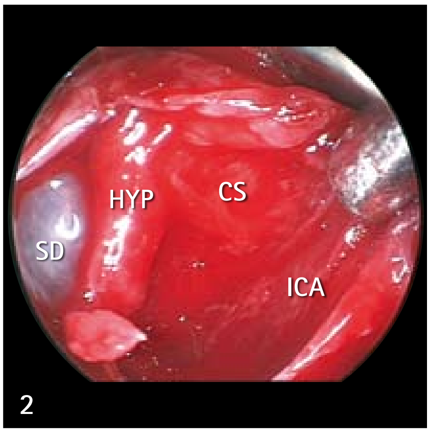


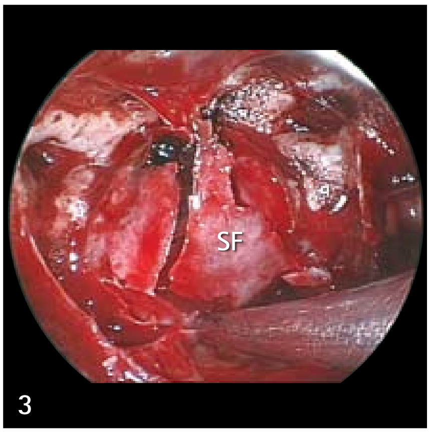


**Fig. 57** *Sellar steps of the biportal approach.*

1. *The tumor removal is performed in a bimanual way using microsuirgical instruments, the endoscope is fixed in the opposite side.*
2. *According to the extended field of view of the endoscope, hidden parts of the surgical field can be observed absolutely. In this way, in comparison with the blind tactile tumor removal, the endoscopic surgeon is able to see pathoanatomical details which are always hidden for the microsurgical resection. Note the diaphragma sellae, pituitary gland, cavernous sinus and the left carotid artery.*
3. *After tumor resection gealfoam is used for tamponade of the tumor bed. Note reconstruction of the bony sellar floor. After leaving the sphenoid sinus, both nasal cavities are inspected and cleansed of coagulated blood; nasal tamponade is not necessary and therefore not recommended.*

## Indication for intraoperative neuronavigation

As discussed above, anatomical landmarks allow safe orientation during endoscopic endonasal surgery. Additional but not essential employment of a C-arm may provide further verification for an exact and delicate dissection; it can be helpful especially during the learning curve. However, in some cases the intranasal anatomy is confusing causing complicated orientation. Typical situations are a conchal sella (problematic orientation), extended tumors with parasellar, transsphenoidal or intranasal expansion (no anatomical alignment), hormonal active microadenomas (extensive bleeding), and re-do surgeries (perplexing scarring of the sellar floor). In these cases, the intraoperative use of a navigation device is recommended and frequently essential to avoid damage to neurovascular structures.

**Fig. 58** *Monitor of the neuronavigation tool by treatment of a recurrent hormonal active microadenoma. In the case of confused anatomy, especially by re-do surgery, navigation offers additional safety.*

**Fig. 59** *Preparation for navigation guided transsphenoidal surgery. Note positioning and fixation of the head allowing trouble-free use of the equipment (BrainLAB AG, Feldkirchen, Germany).*

# Illustrative Cases

## Case 1

### Background

This 41-year-old female suffered from lethargy and decreased libido. The initial examination included hormonal investigation which revealed signs of corticoid malfunction. Detailed endocrinological function tests showed complete insufficiency of the corticotropic, thyrotropic and gonadotropic axes. An MRT scan excluded a tumor; however, an intrasellar cystic lesion could be detected with obvious compression of the pituitary gland (Fig. 60). There was no visual deficit.

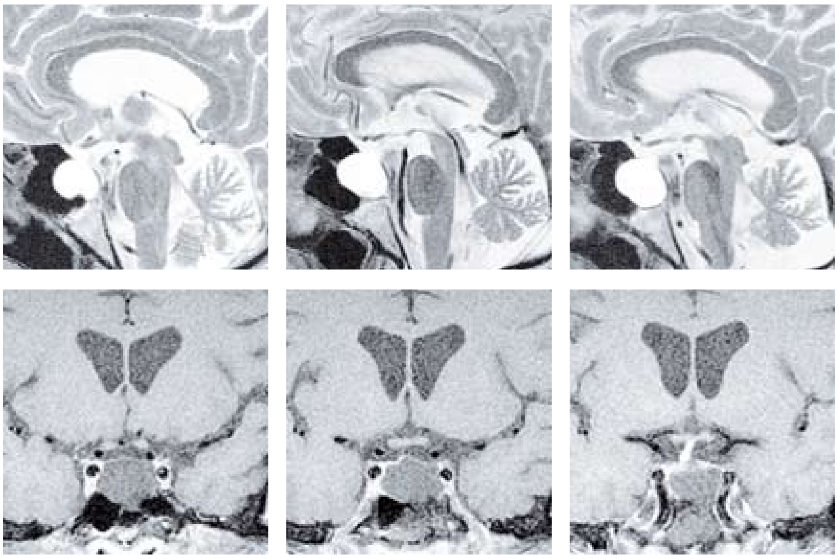

**Fig. 60** *T2w MR imaging in the sagittal plane and contrast medium enhanced wT1 scans in the coronar plane showing an intrasellar cystic lesion. Note the space occupying effect on the coronar scans causing severe compression of the pituitary gland and displacement of the stalk.*

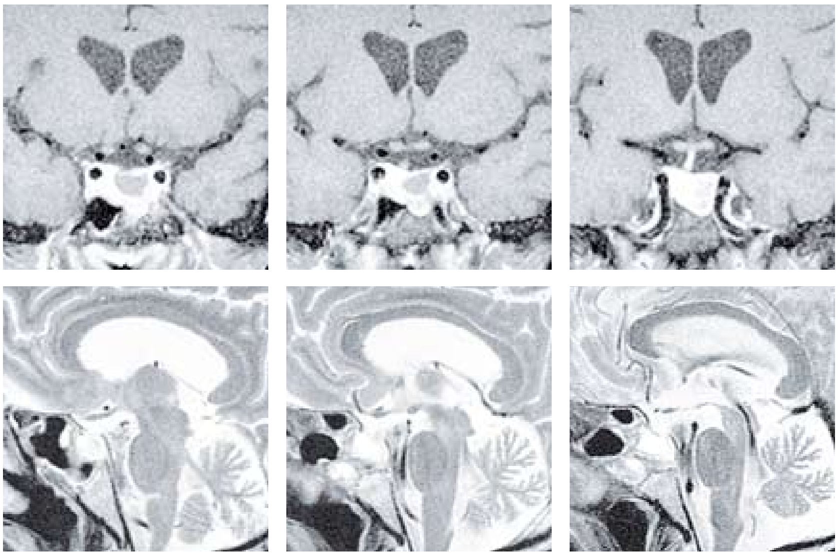

**Fig. 61** *Postoperative imaging showing effective decompression of the pituitary gland.*

**Fig. 62** *Intraoperative photographs. After completion of the binostril approach, the thin bony floor of the sella was opened with a diamond drill; note the useful help of the intraoperative X-ray indicating the optimal placement of opening (A). The wall of the cystic lesion was opened with a microscissor and small parts were sent for histopathological investigation (B). After sufficient opening, the endoscope was entered into the cyst, visualizing the diaphragma sellae, medial wall of the left cavernous sinus and the left intracavernous carotid artery (C). The right carotid was covered with the reddish thin tissue of the pituitary gland (D). After decompression of the cyst, the sellar floor was reconstructed with gelfoam; because of the short and atraumatic surgery without transseptal dissection, no nasal package was used.*

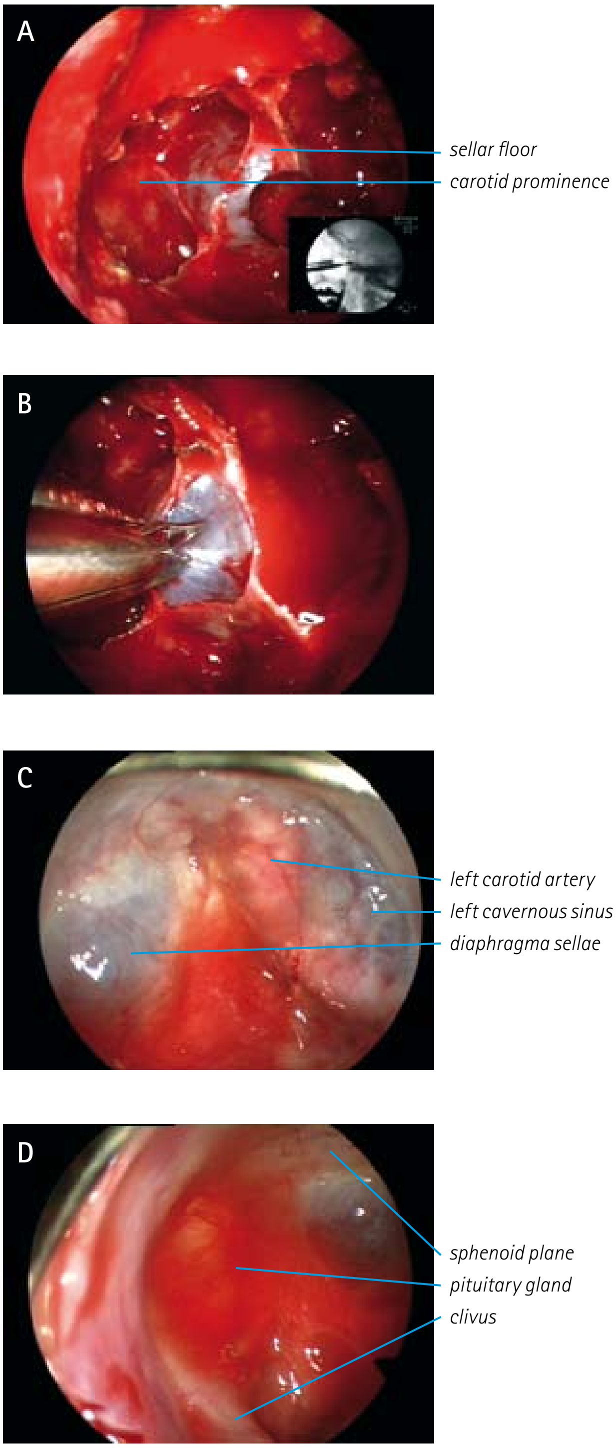


## Postoperative course

The patient made an uneventful recovery with no nasal airflow problems. No visual disturbances occurred; 2 weeks after discharge, the patient could start a 4-week holiday without any restrictions. Three months after surgery, an MRI scan showed effective decompression of the cyst and with an increased volume, the pituitary gland could be clearly seen (Fig. 61). Endocrinological testing showed recovery of corticoid function; however, thyrotropic and gonadotropic functions did not improve.

## Case 2

### Background

A 38-year-old male presented with markedly visual deterioration. Ophthalmological investigation showed bitemporal hemianopia but an MRI scan provided the diagnosis by identifying a large pituitary tumor with intra- and suprasellar extension and severe compression of the optic chiasm (Fig. 63). Despite good clinical tolerance, endocrinological investigation showed a complete lack of adenohypophyseal function.

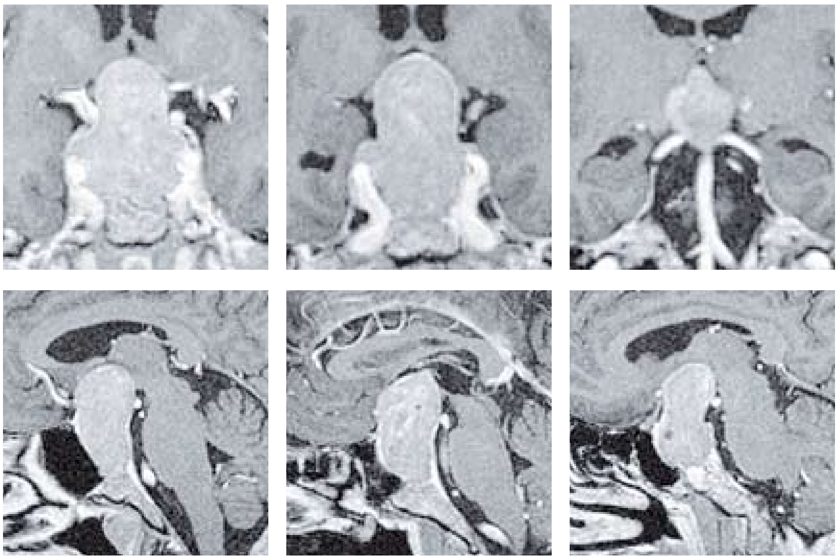

**Fig. 63** *Preoperative T1w imaging after contrast medium in the coronar and sagittal plane showing a pituitary tumor with large suprasellar extension and compression of the optic chiasm.*

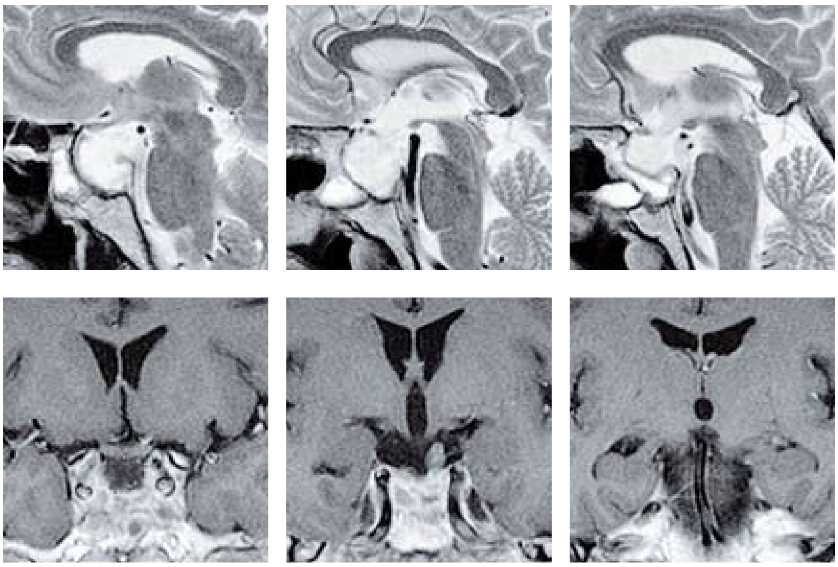

**Fig. 64** *Postoperative T2w sagittal and contrast enhanced T1w coronar imaging revealing complete resection of the tumor.*

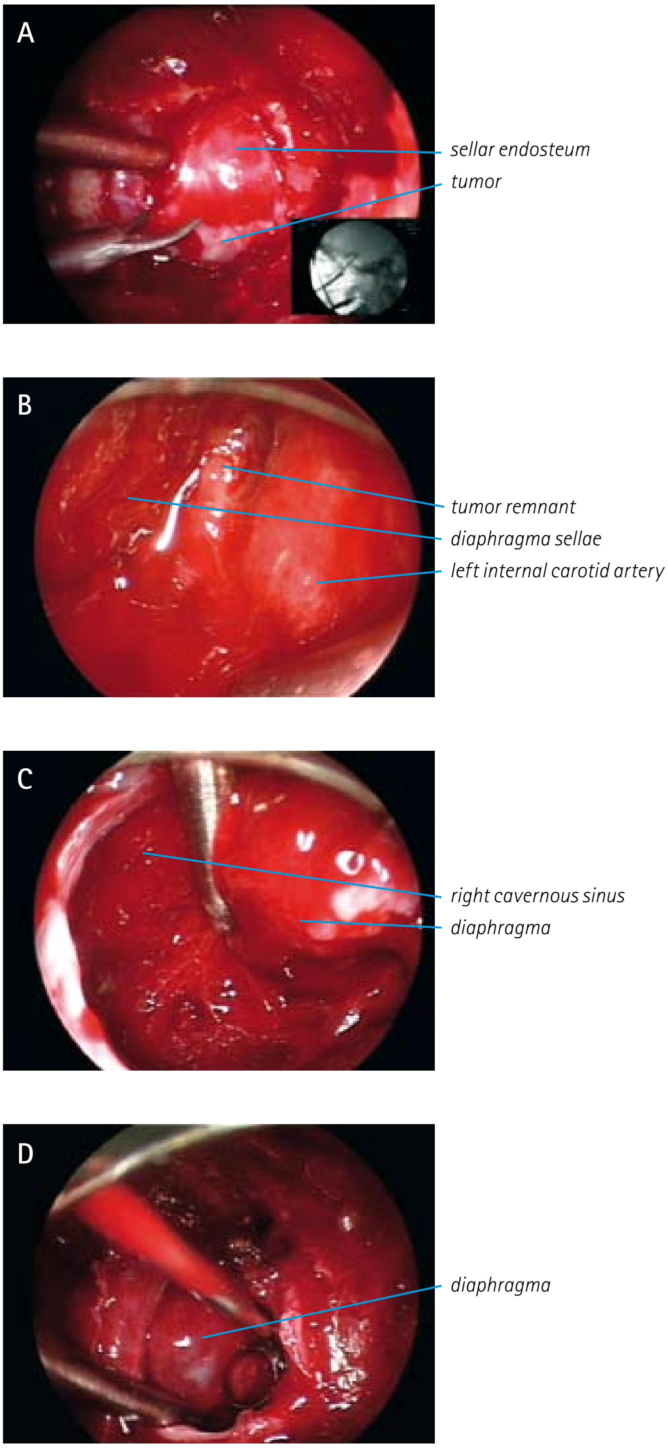


**Fig. 65** *Intraoperative photographs. The sphenoid sinus was explored via a biportal approach; the thin sellar floor was opened with Kerrison punches and the endosteum was incised (A). Note intraoperative use of the C-arm controlling the optimum approach. At first, the clival part of the tumor was removed avoiding early sinking of the diaphragma; thereafter, the laterally located tumor parts were removed on both sides. The endoscopic image allowed ideal visual control of tumor resection with direct observation of the intracavernous carotid artery (B, C). Note a small tumor remnant within the angle between the left carotid artery and diaphragma sellae. After basal and bilateral dissection, the patient was replaced in the Trendelenburg position and the PEEP was increased. Due to this non-invasive increase in intracranial pressure, the suprasellar tumor deflated making careful mobilization possible (D). Without injury to the diaphragma sellae, the sellar floor was reconstructed using gelfoam; implantation of abdominal fat tissue was not necessary. No nasal package was used.*

## Postoperative course

After surgery, visual problems improved immediately. Postoperatively, the patient reported a transient anosmia; however with complete recovery after 6 weeks. Three months after surgery, the bitemporal hemianopia disappeared completely and an MRI scan showed effective decompression of the optic chiasm without evidence of residual tumor tissue (Fig. 64). Pituitary function did not normalize completely; however, after hormonal substitution the patient could return to his previous employment without any restrictions.

## Case 3

### Background

A 46-year-old patient complained of vertigo and headache. An MRI scan was performed and a meningeoma of the tuberculum sellae was detected as a coincidental finding (Fig. 66). Ophthalmological and endocrinological investigations showed no abnormalities. The coronar plane showed no extension of the tumor laterally from the supraclinoid carotid artery. The sagittal plane revealed a tumor matrix behind and below the tuberculum sellae making complete resection via a transcranial approach difficult. After careful analysis of the diagnostic images including three-dimensional planning of procedure (Fig. 67), a decision was made to undertake transsphenoidal exploration.

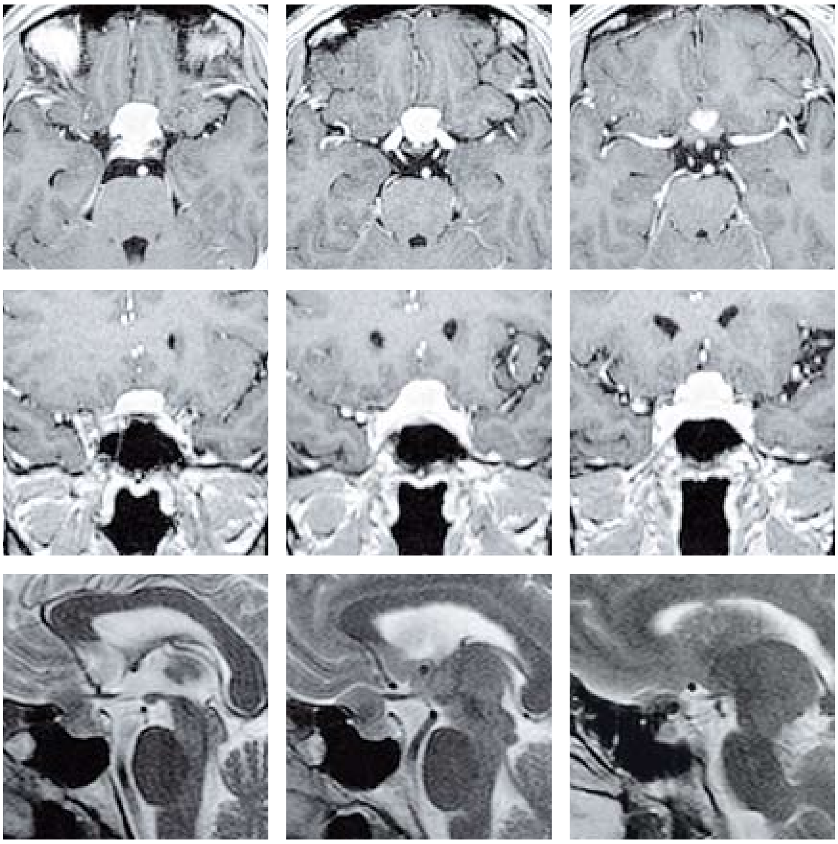

**Fig. 66** *Preoperative imaging of a meningeoma of the planum sphenoidale. The postcontrast axial and coronar T1w pictures show no extension of the tumor laterally from the supraclinoid carotid artery. The sagittal T2w images reveal a tumor matrix behind and below the tuberculum sellae making complete resection via a transcranial approach questionable and transsphenoidal exploration achievable.*

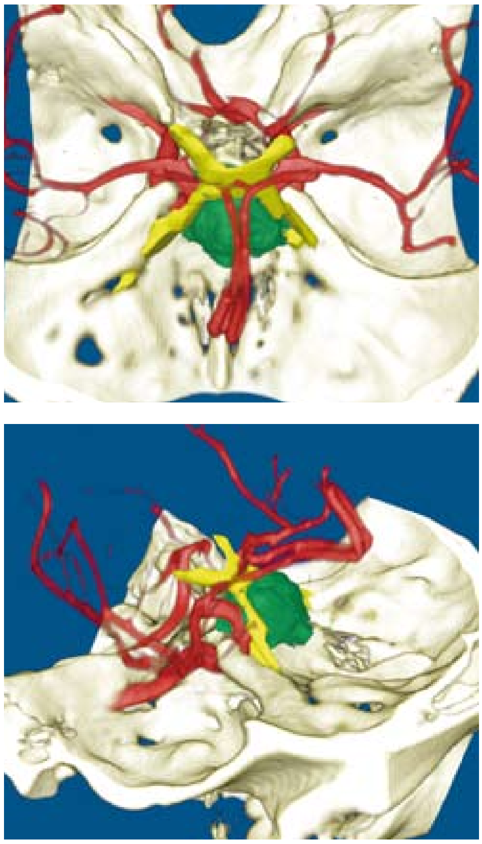

**Fig. 67** *Three-dimensional imaging of the lesion using Dextroscope (Volume Interactions, Singapore). With the help of virtual reality, the optimum approach could be determined.*

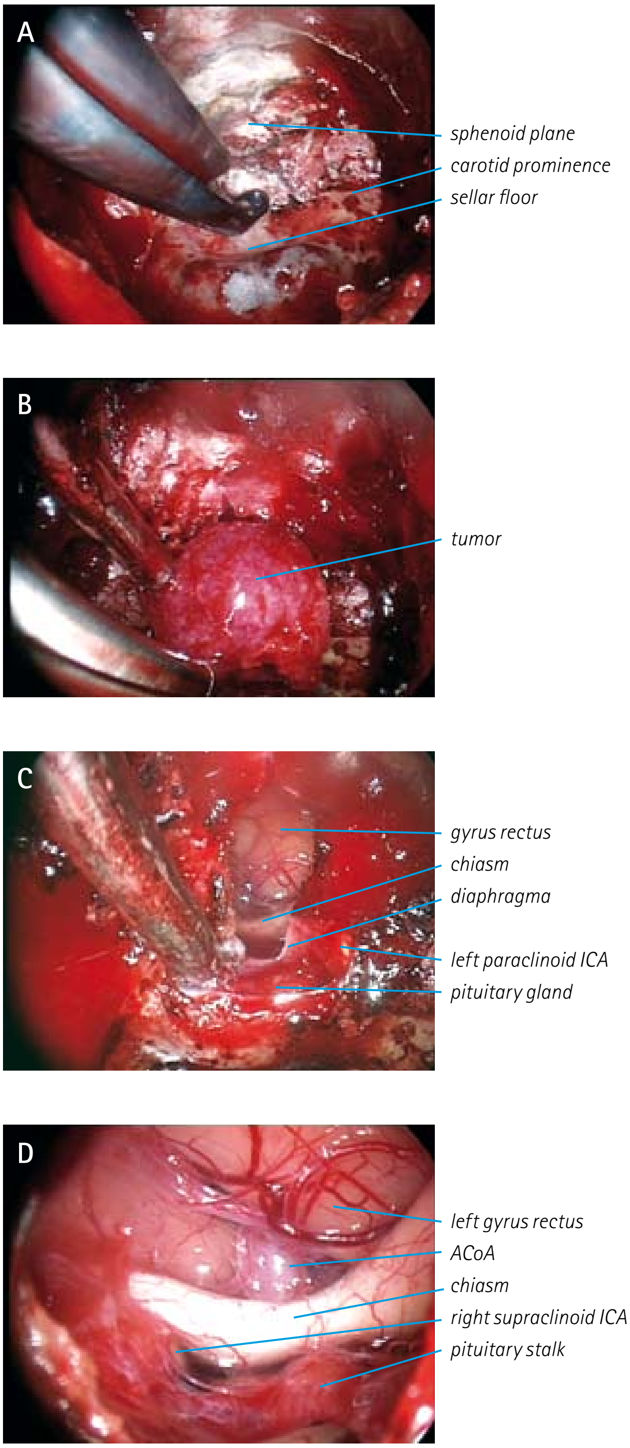


**Fig. 68** *Intraoperative photographs. For adequate transsphenoidal exposure of the planum sphenoidale and tuberculum sellae, the biportal exposure was extended with removal of the right middle turbinate and partial removal of both superior turbinates. The planum sphenoidale and the sellar floor were removed with a diamond drill, the tuberculum sellae with fine Kerrison punches (A). After bone removal, the dura was incised according to the midline and the anterior cranial fossa was opened. The well vascularized tumor was carefully dissected and mobilized from the chiasm without affecting the optic nerves (B). After removal of the intracranial meningeoma, a tumor was found below the diaphragma sellae (C). This part could be successfully dissected from the paraclinoid carotid artery and from the pituitary gland allowing complete tumor resection without involving the intracranial neurovascular structures (D). After tumor dissection, the dural opening was closed in a sheet-by-sheet fashion using DuraGen® collagene matrix graft (Integra, Plainsboro, New Jersey, USA) and fascia lata.*

**Postoperative course**

The direct postoperative course was uneventful (Fig. 69). The intraoperative lumbar drain could be removed on the 3rd day after surgery and the patient could be discharged in a good physical condition without visual disturbances. However, 4 weeks after surgery, a nasal CSF leak occurred, making re-operation necessary. After the second intervention, the patient showed normal recovery and could return to his previous employment. Three months after surgery, an MRI scan showed no residual tumor and ophthalmological and hormonal investigations were normal (Fig. 70).

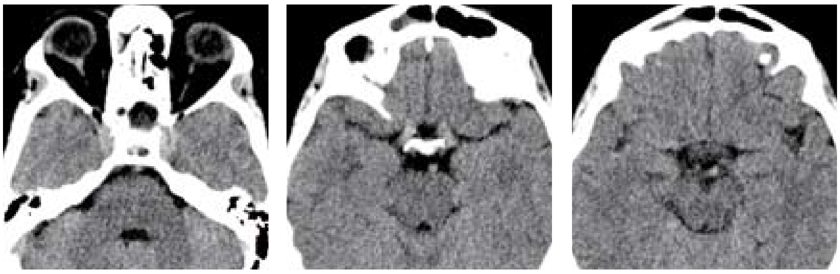

**Fig. 69** *CT scan on the first postoperative day showing no postoperative comloications.*

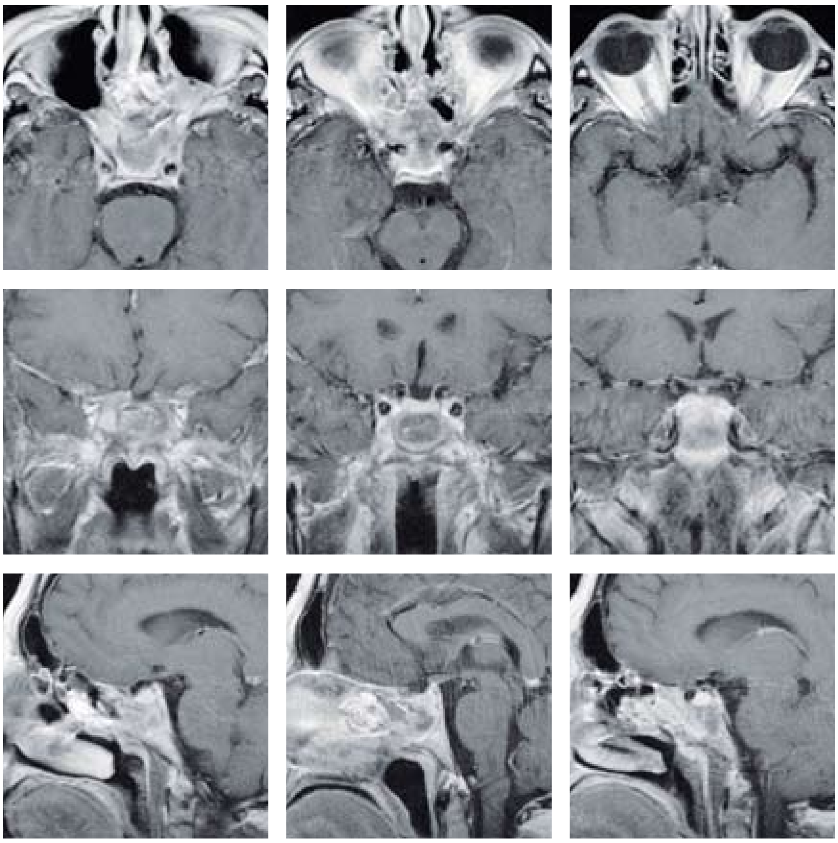

**Fig. 70** *MRI three months postoperatively revealing complete resection of the tumor.*

## TRanssphenoidal ENDoscopy: the TREND-setting equipment

Considering recent publications on transsphenoidal surgery, it will be clear: TRanssphenoidal ENDoscopy is TREND-setting! Nevertheless, the endoscopic technique is not in routine use everywhere and neurosurgeons are often reluctant to use it. The cause of the aversion is the steep learning curve. Permanent contamination of the endoscope with blood and nasal secretions causes difficult orientation and without a nasal speculum, the endonasal dissection is mysterious for neurosurgeons. In addition, the para-endoscopic and biportal dissection is very unfamiliar. The first frustrating steps add to the growing impatience of surgeons who then give up the further education.

Pre-conditions of transsphenoidal endoscopy are the basic endoscopic experience and anatomical studies in the laboratory; however, it is undisputable that a newly developed endoscope should shorten the unacceptable learning phase.

The endoscope for transsphenoidal skull base surgery must combine a brilliant optical feature with a practical and user-friendly application during surgery. To complete the requirements, the following details are essential:

1. Superior optical quality;
2. Optimal suction-irrigation channel;
3. Ergonomic grasping part;
4. Sufficient length for extended transsphenoidal approaches;
5. Connection to a holding device;
6. Connection to a navigation device.

1. To obtain a brilliant image quality, the TREND endoscope was meticulously redeveloped (Fig. 71). The high-quality endoscope with a 4 mm diameter offers an undisturbed, true color and highly realistic image of structures. For unproblematic visualization of hidden parts of the surgical field, a variable application of 0° and 30° endoscopes is available.

2. In transsphenoidal surgery, most used endoscopes do not provide adequate suction and irrigation. However, when using a pure endoscopic approach without a nasal speculum, the tip of the instrument is permanently contaminated with blood and mucosal secretions limiting the surgeon's patience. In addition, continuous removal and introduction of the endoscope invokes additional damage to the nasal mucosa. Based on lengthy experience the TREND endoscope was developed with an effective irrigation and suction device (Fig. 72). The continuous suction avoids fogging of the endoscope in the warm and wet nasal cavity and immediately removes

**Fig. 71** *Photograph showing the Aesculap TREND pituitary endoscope with a 4 mm diameter offering an undisturbed, true color and highly realistic image of structures. For direct visualization of hidden parts of the surgical field, a variable application of 0° and 30° endoscopes is available. For approaching deep-seated lesions, an effective length of the endoscope has been defined.*

**Fig. 72** *Photographs demonstrating the ergonomic grasping part of the endoscope. An efficient suction – irrigation device is incorporated where the valve is controlled simply with the index finger. In addition, the grasping part offers a quick connection of the endoscope to a holding arm and navigation device.*

vapour and smoke. The intermittent irrigation can be effectively controlled with the index finger offering useful additional cleaning of the optics and flushing the surgical field. An essential and undisputable advantage of the TREND equipment!

3. Difficulties in the learning curve of transsphenoidal endoscopy are also caused by an additional problem, namely by poor handling of endoscope systems. The uncomfortable handling causes uncontrolled and rough movements within the sensitive surgical field and, in addition, is tiring for the surgeon. The TREND endoscope effectively compensates this drawback with a human-engineered grasping part. The surgeon holds the TREND endoscope as a fine microinstrument and not like a "forceful pistol" allowing precise manipulation (Figs. 72, 73). The efficient suction – irrigation device is also incorporated within the grasping part where the valve is controlled simply with the index finger. Moreover, the unique construction and perfect balance of the TREND endoscope provide a less tiring tool for the neurosurgeon. In addition, the grasping part offers a quick connection of the endoscope to a holding arm (Fig. 74).

4. The newly developed TREND endoscope should be able to meet the demands of extended skull base approaches. For approaching deep-seated lesions, an effective length of the endoscope has been defined: it is not too long avoiding inefficient handling, but long enough to reach intradural targets.

5. The need for bi-manual dissection in the deep-seated surgical field is essential especially during complicated skull base surgery. Therefore, after completing the biportal-binostril approach, the endoscope can be easily fixed in a special holding arm. The endoscope placed through the other nostril does not disturb surgical dissection (Figs. 74, 75).

6. As mentioned above, surgical orientation can, in some cases, be highly confusing. The absence of anatomical landmarks within the sphenoid sinus caused by a conchal sella, an extended tumor growing into the sphenoid sinus and nasal cavity or severe scarring after previous surgery are the most typical problems of hindered orientation making intraoperative use of neuronavigation necessary. The special construction of the TREND endoscope allows easy and uncomplicated connection to several navigation systems: the tip of the endoscope can then be steered with safe control of the surgical approach (Fig. 76).


**Fig. 73** *Intraoperative application of the TREND endoscope approaching the nasal cavity. The surgeon remains beside the patient in an ergonomic way and has optimal control of the endoscopic monitor (A). Using the ergonomic grasping part the surgeon holds the TREND endoscope as a fine microinstrument and not like a „forceful pistol" allowing precise manipulation. Moreover, the unique construction and perfect balance of the TREND endoscope provide a less tiring tool for the neurosurgeon. According to the paraendoscopic dissection instruments with a straight, non-bayonet design can be used (B). Note the use of a special manufactured bipolar coagulator (C).*

**Fig. 74** *After performing the biportal binostril approach, the endoscope is connected with a holding device, the grasping part offers a quick fixation of the endoscope in a quick and user-friendly way (A, B, C, D).*



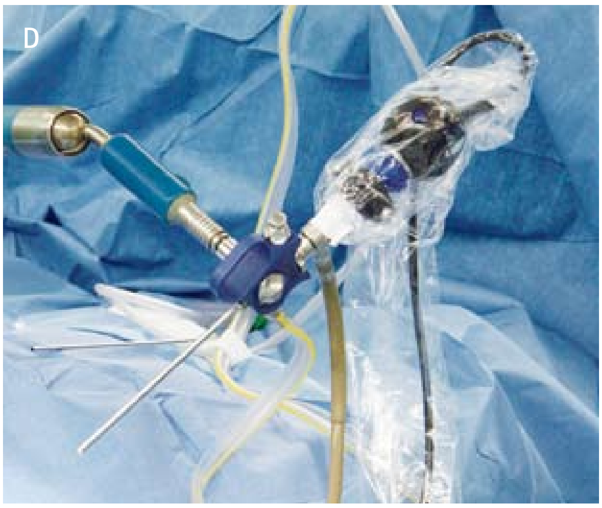


**Fig. 75** *The endoscope is fixed through the left nostril, the surgery is continued through the right nasal cavity. The biportal approach offers free introduction and improved bimanual manoeuvrability of the surgical instruments without using a nasal speculum. In this way, the TREND endoscope for transsphenoidal skull base surgery combine a brilliant optical feature with a practical and user-friendly application during surgery.*

**Fig. 76** *Intraoperative photographs showing the application of a BrainLAB navigation device connected to the pituitary endoscope.*

# Abbreviations

| | |
|---|---|
| BA | basilar artery |
| CL | clivus |
| CN I | olfactory nerve |
| CN II | optic nerve |
| CN III | oculomotor nerve |
| CN IV | trochlear nerve |
| CN V/1 | opthalmic nerve |
| CN VI | abducent nerve |
| CP | carotid prominence |
| CS | cavernous sinus |
| EP | epipharynx |
| GL | Grubert's ligament |
| HYP | pituitary gland |
| ICA | internal carotid artery |
| IT | inferior turbinate |
| MS | maxillary sinus |
| MT | middle turbinate |
| NS | nasal septum |
| OC | oral cavity |
| OP | optic prominence |
| PCoA | posterior communicating artery |
| SA | septal artery |
| SD | sellar diaphragm |
| SF | sellar floor |
| SP | sphenoid planum |
| SS | sphenoid sinus |
| ST | superior turbinate |
| TA | tuba auditiva |
| TT | torus tubarius |
| TU | tumor |

# MINOP® TREND

FH615

MINOP® TREND ergonomic grasping handle with irrigation button

FH610R

MINOP® TREND irrigation/suction trocar for 0° endoscope PE487A
diameter: 4.5/6.0 mm, working length: 120 mm

FH611R

MINOP® TREND irrigation /suction trocar for 30° endoscope PE507A
diameter: 4.5/6.0 mm, working length: 120 mm

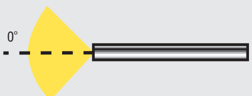


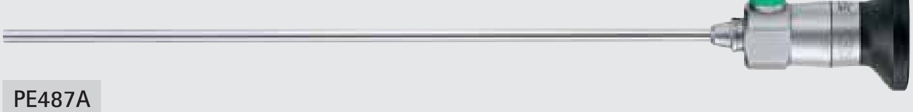

PE487A

MINOP® TREND endoscope
Dircetion of view 0°
Shaft diameter 4.0 mm

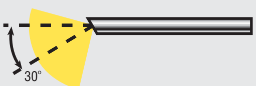


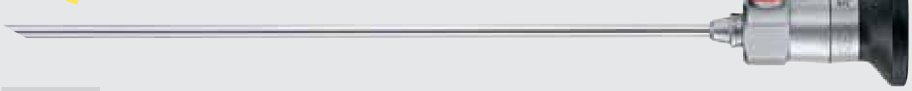

PE507A

MINOP® TREND endoscope
Direction of view 30°
Shaft diameter 4.0 mm

For more neuroendoscopes, see www.aesculap-neuro.com or "Neuroendoscopy Catalogue" C35502.

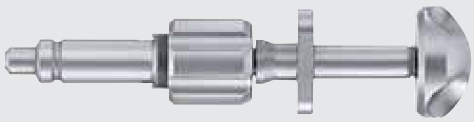

**RT099R**

MINOP® TREND adapter for quick and user-friendly connection with Aesculap holding device

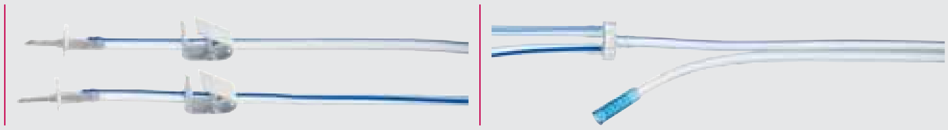

**FH605SU** 4.0 m

MINOP® TREND irrigation/suction tube, sterile
for MINOP® TREND handle FH615 or MINOP® TR trocar FH601R,
with 2 puncture needles

Sales unit:
**PAK** = Package of 10 tubes

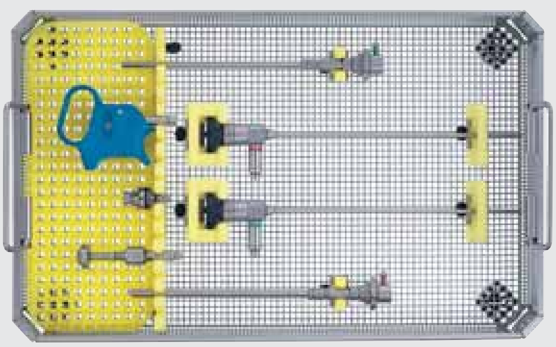

**FF357R**

MINOP® TREND storage rack
with silicone cushioning rack and lid
for all MINOP® TREND components
(instruments not included)

Container for
MINOP® storage rack FF357R
consisting of:

| | |
|---|---|
| **JK740** | Container bottom |
| **JK789** | Container lid (basic version) |

For more neuroendoscopes, see www.aesculap-neuro.com or “Neuroendoscopy Catalogue” C35502.

# TREND Pituitary Instruments

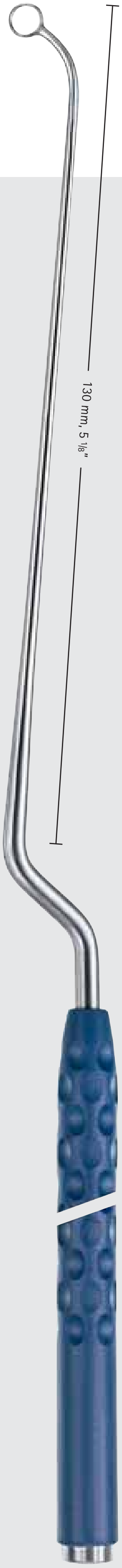


1/1

Bayonet design with ergonomic grasping part and semi-sharp tips

1/1

| NICOLA | NICOLA | HARDY | HARDY | HARDY | HARDY | HARDY | HARDY |
|---|---|---|---|---|---|---|---|
| FA041R | FA042R | FA043R | FA044R | FA045R | FA046R | FA047R | FA060R |
| Curette 6.5 mm | Curette 6.5 mm | Enucleator left cutting | Enucleator right cutting | Curette 4.0 mm | Curette 4.0 mm | Curette 4.0 mm | Curette 4.0 mm |
| 45° vertical angled long neck | 45° horizon-tal angled short neck | | | 90° left angled long neck | 90° left angled short neck | 90° right angled long neck | 90° right angled short neck |

1/1

| HARDY | HARDY | HARDY | HARDY | HARDY | HARDY | REULEN-LANDOLT | REULEN-LANDOLT |
|---|---|---|---|---|---|---|---|
| FA061R | FA062R | FA063R | FA064R | FA065R | FA066R | FA067R | FA068R |
| Curette 4.0 mm | Curette 4.0 mm | Curette 6.0 mm | Curette 6.0 mm | Curette 6.0 mm | Curette 6.0 mm | Micro Hook 1.7 mm | Dissector 2.0 mm |
| 45° left horizontal angled short neck | 45° right horizontal angled short neck | 90° left angled long neck | 90° left angled short neck | 90° right angled long neck | 90° right angled short neck | | blunt |

**FA041R-FA068R**

Working length: 130 mm, 5 ⅛"
Total length: 280 mm, 11"

For more pituitary instruments, see www.aesculap-neuro.com or "Neurosurgery Catalogue" C20102.

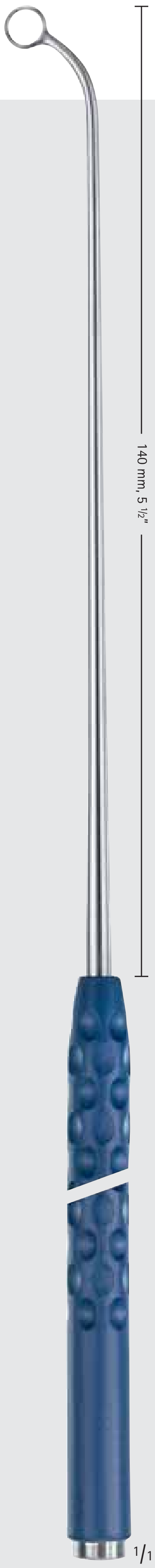


Straight design with ergonomic grasping part and semi-sharp tips

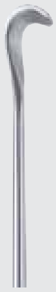

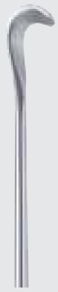

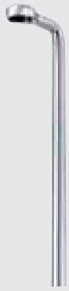


NICOLA
**FA030R**
Curette
6.5 mm
45° vertical angled long neck

NICOLA
**FA031R**
Curette
6.5 mm
45° horizontal angled short neck

HARDY
**FA032R**
Enucleator
left cutting

HARDY
**FA033R**
Enucleator
right cutting

HARDY
**FA034R**
Curette
4.0 mm
90° angled long neck

HARDY
**FA035R**
Curette
4.0 mm
90° angled short neck


HARDY
**FA036R**
Curette
4.0 mm
45° angled short neck

HARDY
**FA037R**
Curette
6.0 mm
90° angled long neck

HARDY
**FA038R**
Curette
6.0 mm
90° angled short neck

LANDOLT-REULEN
**FA039R**
Micro Hook
1.7 mm

LANDOLT-REULEN
**FA040R**
Dissector
2.0 mm
blunt

**FA030R–FA040R**
Working length: 140 mm, 5 ½"
Total length: 265 mm, 10 ½"

For more pituitary instruments, see www.aesculap-neuro.com or "Neurosurgery Catalogue" C20102.

# TREND Pituitary Instruments

PAPAVERO-CASPAR

| | |
|---|---|
| FF589R | 80 x 11 mm |
| FF590R | 90 x 13 mm |
| FF591R | 100 x 15 mm |

Slim profile and lightweighted specula
Not recommended for biportal endoscopic approach

| | |
|---|---|
| FF590B | 90 x 13 mm |

NOIR®
Coated specula
Not recommended for biportal endoscopic approach

| | |
|---|---|
| OK090R | 90 x 7 mm |

Nasal specula for protective mobilization of the turbinates

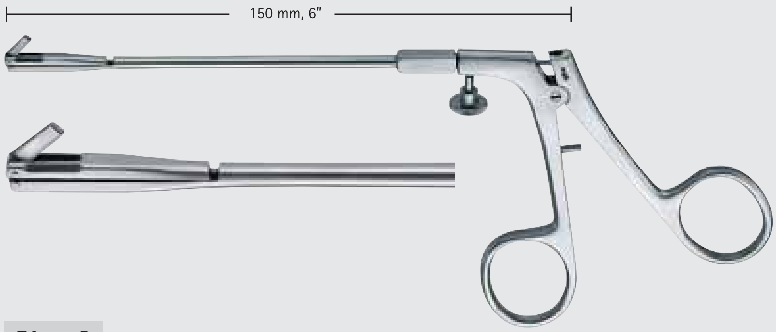


| |
|---|
| FA076R |

Backwards cutting antrum punch, rotating sheath 360°, working length, 120 mm , 4 ¾"
For removal of posterior nasal septum

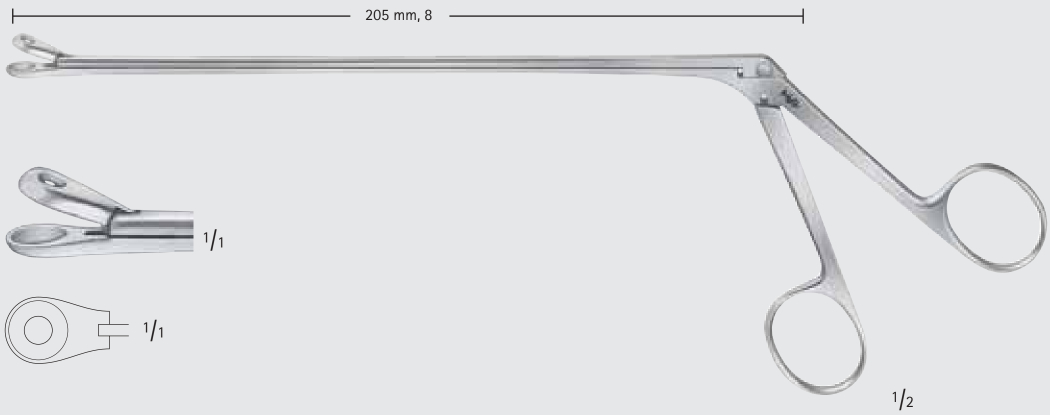


LANDOLT

| | |
|---|---|
| FF345R | Diam. 9.0 mm |

Tumor grasping forceps, blunt

For more pituitary instruments, see www.aesculap-neuro.com or "Neurosurgery Catalogue" C20102.

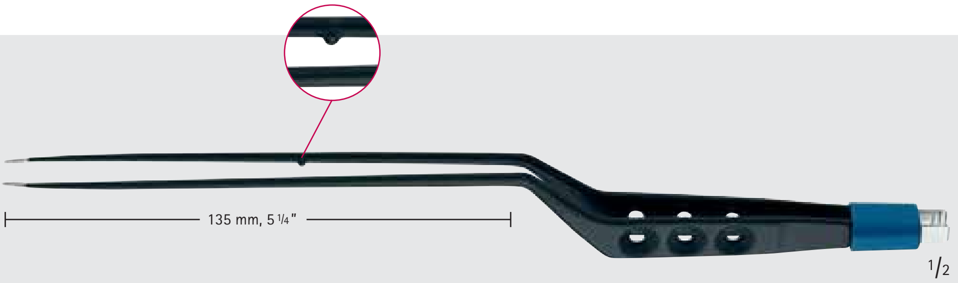


**GK801R**

Bipolar coagulation forceps with slender jaws and higher spring tension

250 mm, 10"

Special pin between the branches opens the tip of the forceps by additional compression of the handle – allowing secure coagulation in narrow and deep seated surgical field.

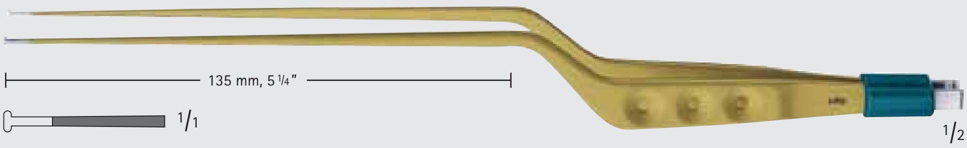


**GK800R**

T-coagulation forceps with blunt, t-shaped tips

255 mm, 10"

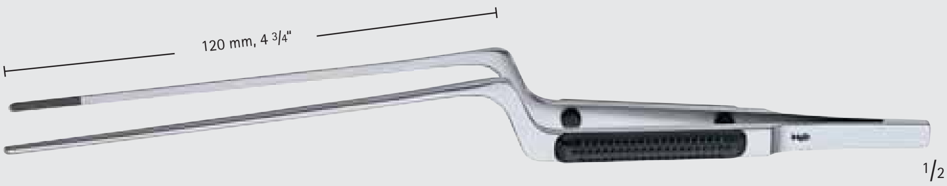


**FM158R**

Bayonet grasping forceps straight tip

245 mm, 9 3/4"


| | |
|---|---|
| Jaw | |
| 0.5 mm | **FM156R** |
| 0.9 mm | **FM157R** |
| Jaw length | 120 mm, 4 3/4" |
| Total length | 240 mm, 9 1/2" |

Bayonet micro grasping forceps straight tip

For more pituitary instruments, see www.aesculap-neuro.com or "Neurosurgery Catalogue" C20102.

# TREND Pituitary Instruments

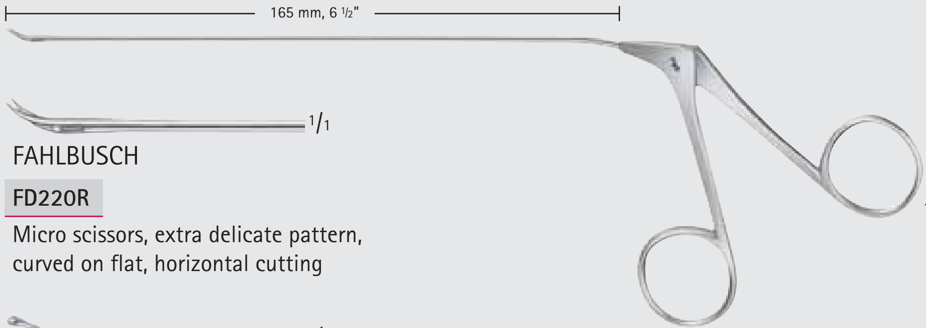


1/2

1/1

FAHLBUSCH

**FD220R**

Micro scissors, extra delicate pattern,
curved on flat, horizontal cutting

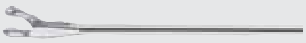

1/1

1/1

NICOLA

**FD222R** Diam. 2.5 mm

Forceps, scoop-shaped

1/1



1/1

YASARGIL-NICOLA

**FD224R**

Grasping forceps with long
conical jaw

1/1

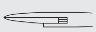

1/1

NICOLA

**FD226R** Diam. 2.5 mm

Micro scissors, straight

**FD220R–FD226R**

extra delicate tubular shaft scissors and grasping
instruments for pituitary & skull base surgery

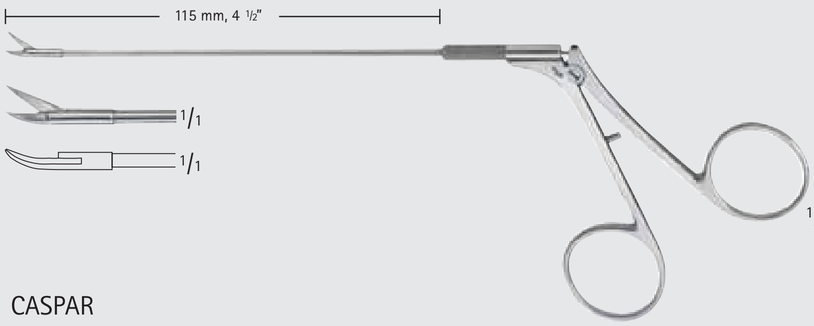


1/2

1/1

1/1

CASPAR

**FD228R**

Micro scissors, curved
rotatable sheath 360°

For more pituitary instruments, see www.aesculap-neuro.com or "Neurosurgery Catalogue" C20102.


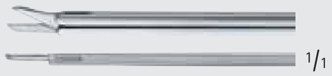


**FA072R**
straight

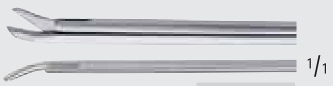


**FA073R**
left curved

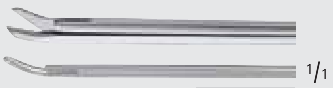


**FA074R**
right curved

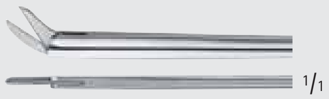


**FA075R**
angular

**FA072R–FA075R**
Micro Scissors

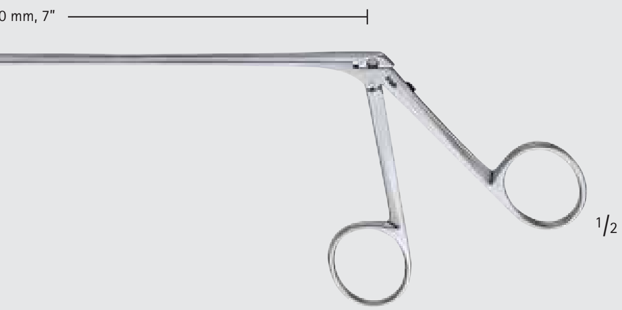


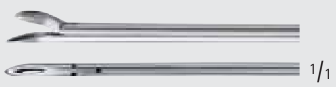


**FA069R**
straight

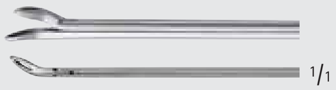


**FA070R**
right curved

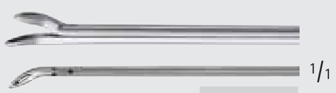


**FA071R**
left curved

**FA069R–FA071R**
Micro Forceps

For more pituitary instruments, see www.aesculap-neuro.com or "Neurosurgery Catalogue" C20102.

# Suction Instruments

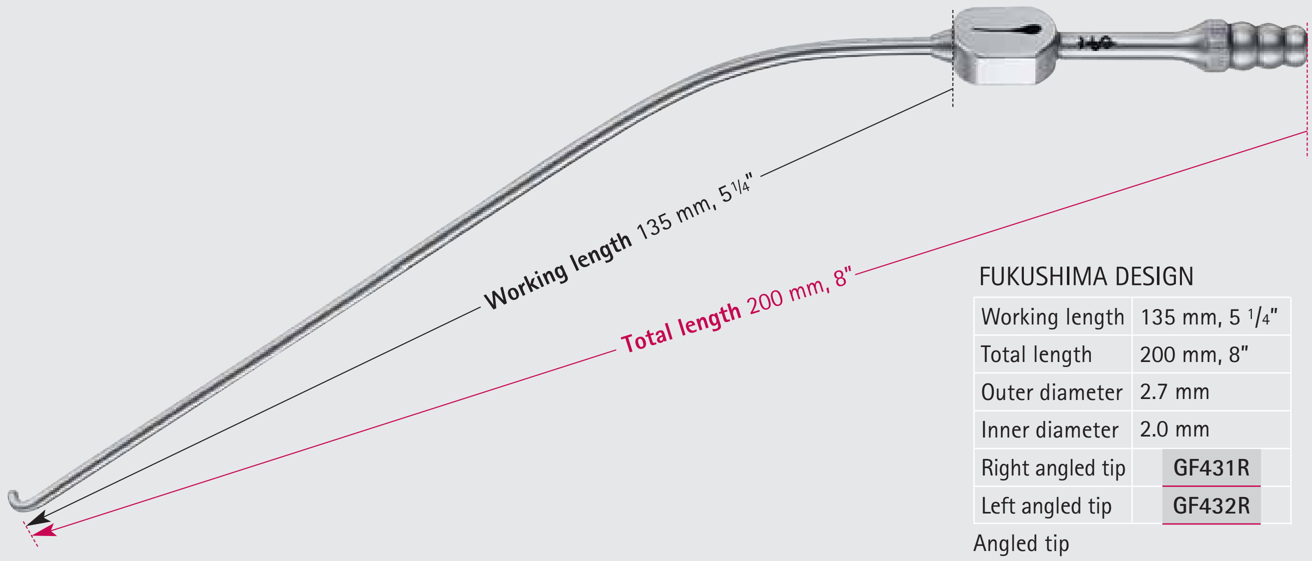


FUKUSHIMA DESIGN

| | |
|---|---|
| Working length | 135 mm, 5 1/4" |
| Total length | 200 mm, 8" |
| Outer diameter | 2.7 mm |
| Inner diameter | 2.0 mm |
| Right angled tip | GF431R |
| Left angled tip | GF432R |

Angled tip

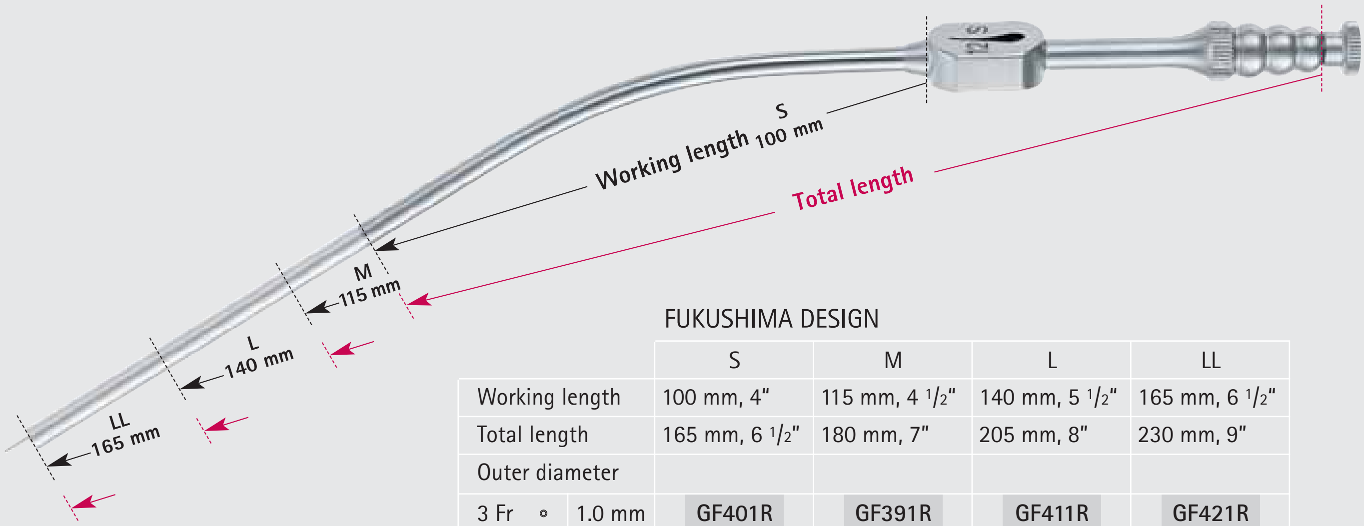


FUKUSHIMA DESIGN

| | | | S | M | L | LL |
|---|---|---|---|---|---|---|
| Working length | | | 100 mm, 4" | 115 mm, 4 1/2" | 140 mm, 5 1/2" | 165 mm, 6 1/2" |
| Total length | | | 165 mm, 6 1/2" | 180 mm, 7" | 205 mm, 8" | 230 mm, 9" |
| Outer diameter | | | | | | |
| 3 Fr | ○ | 1.0 mm | GF401R | GF391R | GF411R | GF421R |
| 4 Fr | ○ | 1.4 mm | GF402R | GF392R | GF412R | GF422R |
| 5 Fr | ○ | 1.7 mm | GF403R | GF393R | GF413R | GF423R |
| 6 Fr | ○ | 2.0 mm | GF404R | GF394R | GF414R | GF424R |
| 7 Fr | ○ | 2.3 mm | GF405R | GF395R | GF415R | GF425R |
| 8 Fr | ○ | 2.7 mm | GF406R | GF396R | GF416R | GF426R |
| 9 Fr | ○ | 3.0 mm | GF407R | GF397R | GF417R | GF427R |
| 12 Fr | ○ | 4.0 mm | GF409R | GF399R | GF419R | GF429R |

For more pituitary instruments, see www.aesculap-neuro.com or "Neurosurgery Catalogue" C20102.

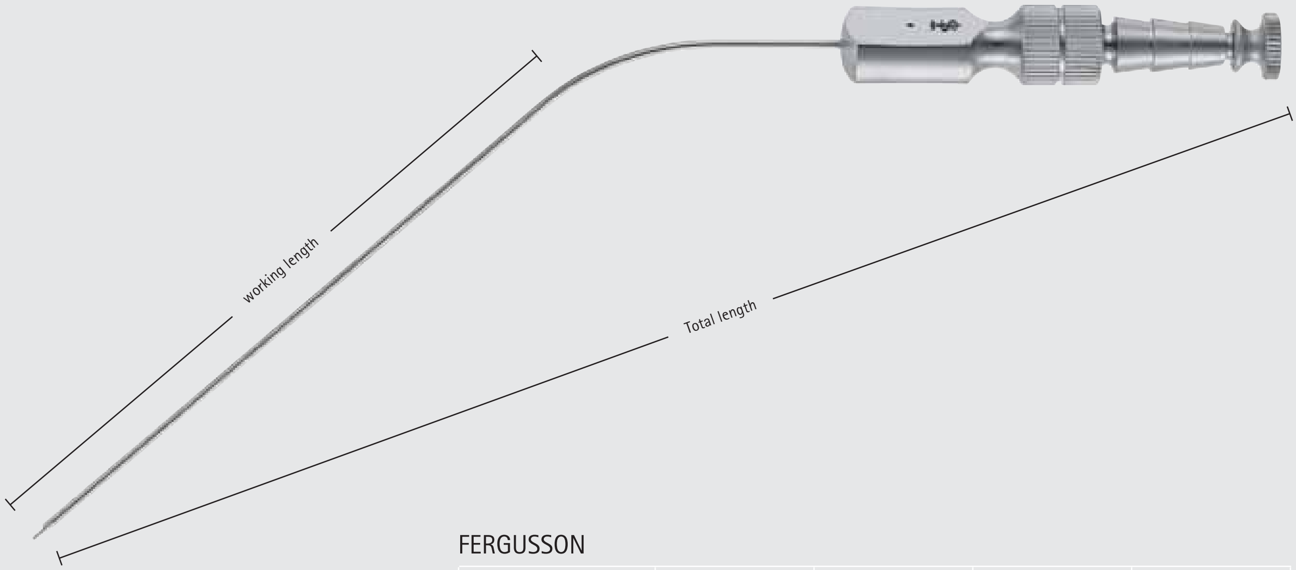


FERGUSSON

| | | | | |
|---|---|---|---|---|
| Working length | 110 mm, 4 3/8" | 130 mm, 5 1/8" | 160 mm, 6 1/4" | 200 mm, 8" |
| Total length | 195 mm, 7 3/4" | 215 mm, 8 1/2" | 245 mm, 9 3/4" | 280 mm, 11" |
| Diam. | | | | |
| 1.5 mm | GF350R | GF360R | GF370R | GF380R |
| 2.0 mm | GF351R | GF361R | GF371R | GF381R |
| 2.5 mm | GF352R | GF362R | GF372R | GF382R |
| 3.0 mm | GF353R | GF363R | GF373R | GF383R |
| 4.0 mm | GF354R | GF364R | GF374R | GF384R |
| 5.0 mm | GF355R | GF365R | GF375R | GF385R |

For more pituitary instruments, see www.aesculap-neuro.com or "Neurosurgery Catalogue" C20102.

# XS Instruments

**Instrument complete, consting of: jaw insert and handle**
**XS instruments with slim tube shaft design for key-hole and transnasal surgery**

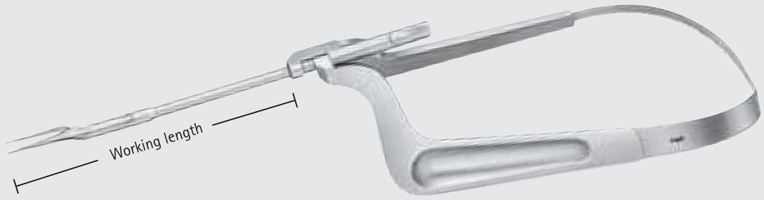


| | | | recommended length for transnasal surgery |
|---|---|---|---|
| Working length | 70 mm, 2 3/4" | 100 mm, 4" | 130 mm, 5 1/8" |
| Total length | 200 mm, 8" | 230 mm, 9" | 260 mm, 10 1/4" |
|  1/1 XS Micro scissors, straight, sharp/sharp | FM670R | FM671R | FM672R |
|  1/1 XS Micro scissors, straight, blunt/blunt | FM690R | FM691R | FM692R |
| 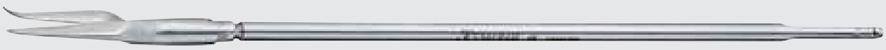 1/1 XS Micro scissors, curved, sharp/sharp | FM680R | FM681R | FM682R |
| 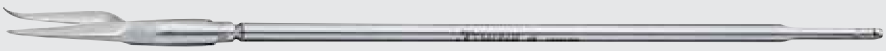 1/1 XS Micro scissors, curved, blunt/blunt | FM700R | FM701R | FM702R |
| 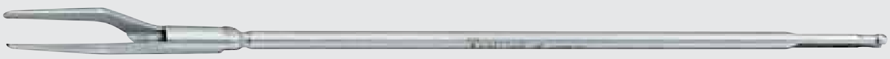 1/1 XS Micro forceps, jaw 0.9 mm | FM710R | FM711R | FM712R |
| 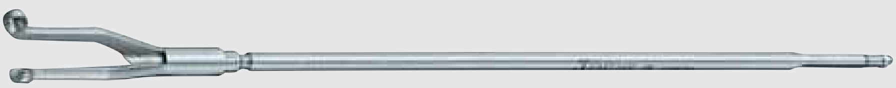 1/1 XS Micro tumor grasping forceps, jaw 3 mm, sharp | FM720R | FM721R | FM722R |

For more pituitary instruments, see www.aesculap-neuro.com or "Neurosurgery Catalogue" C20102.

# Kerrison Bone Punches

NOIR (Non-irritating reflections) Kerrisons are recommended for pituitary and skull base neuroendoscopy

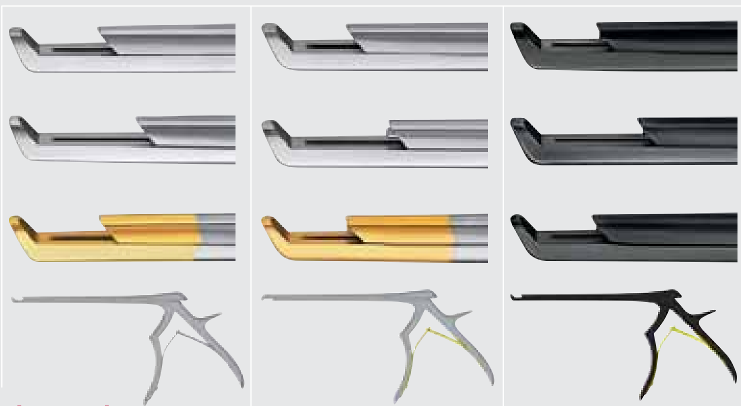

standard footplate

Jaw opening 15 mm

thin footplate

## Jaw position 130°, upward opening

| Shaft length | Width | Footplate | Non detachable, without ejector | Detachable | Ejector | NOIR®, detachable | Ejector | Jaw opening |
|---|---|---|---|---|---|---|---|---|
| 180 mm, 7" | 1.0 mm | thin | FF771R | FK906R | – | FK906B | – | 8 mm |
| | 1.5 mm | thin | FF645R | FK923R | – | FK923B | – | 9 mm |
| | 2.0 mm | thin | FF772R | FK907R | ✔ | FK907B | ✔ | 9 mm |
| | 2.5 mm | thin | FF646R | FK924R | ✔ | FK924B | ✔ | 10 mm |
| | 3.0 mm | thin | FF773R | FK908R | ✔ | FK908B | ✔ | 10 mm |
| | 4.0 mm | thin | FF769R | FK909R | ✔ | FK909B | ✔ | 12 mm |

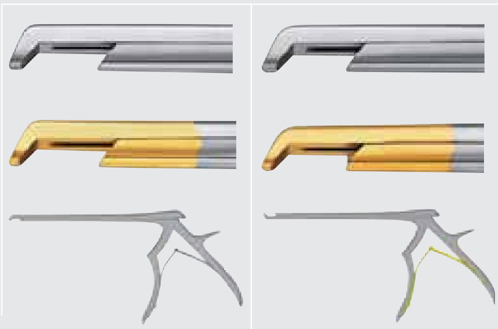

standard footplate

thin footplate

## Jaw position 130°, downward opening

| Shaft length | Width | Footplate | Non detachable, without ejector | Detachable | Ejector | Jaw opening |
|---|---|---|---|---|---|---|
| 180 mm, 7" | 1.0 mm | thin | FF781R | FK936R | – | 8 mm |
| | 2.0 mm | thin | FF782R | FK937R | ✔ | 9 mm |
| | 3.0 mm | thin | FF783R | FK938R | ✔ | 10 mm |
| | 4.0 mm | thin | FF784R | FK939R | ✔ | 12 mm |

For more pituitary instruments, see www.aesculap-neuro.com or "Neurosurgery Catalogue" C20102.

# Holding Arms

**FF168R** **Holding device for neuroendoscopes**

Flexible holding device
with mechanic fixation

- special accessories allow easy and user-friendly connection with every Aesculap endoscope
- simple to assamble onto OR table railing
- fast & sterile set-up in the OR
- all components fully autoclavable

Diam. 20 mm

**RT040R** **UNITRAC®**
Flexible holding device with pneumatic fixation

- UNITRAC®, the universal retraction and holding system with special accessories for neuroendoscopy
- Pneumatically-assisted system for direct connection to OR compressed air supply
- Integrated safety systems prevent collapse of holding arm if OR compressed air supply is interrupted
- Simple to assemble onto the OR table railing
- Single handed use
- Fast and sterile set-up in the OR
- All components fully autoclavable

Diam. 20 mm

**Fixation devices**
**for RT040R and FF168R**

**FF280R** Flexible fixing element with ball joint suitable for RT040R and FF168R

**RT090R** Flexible fixing element with sprocket suitable for RT040R and FF168R

**FF151R** Rigid fixation element suitable for RT040R and FF168R

For more holding devices, see www.aesculap-neuro.com or "Neuroendoscopy Catalogue" C35502.

# Power Systems

## Electric

GD670
microspeed® uni control unit

GD676
microspeed® uni Hi 150
electric high speed motor for all Hi-Line and Hi-Line XS handpieces

## Pneumatic

GA740R
HiLAN® XS pneumatic highspeed motor for
all Hi-Line XS handpieces

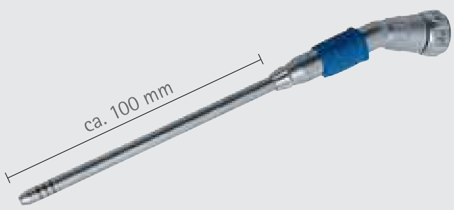


GB758R
Hi-Line XS handpiece, for 100 mm burrs
3 ring code at tip

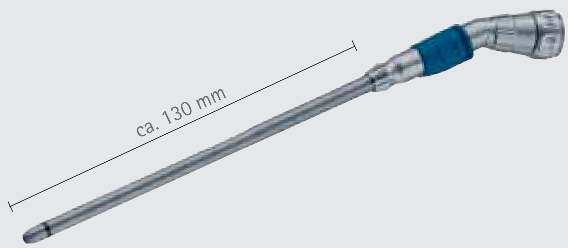


GB771R
Hi-Line XS handpiece, for 130 mm burrs
extra long XL1; 1 bold ring code at tip

**Diamond burr**

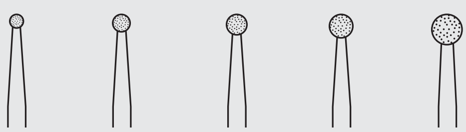

| | length | 1.8 mm | 2.3 mm | 2.7 mm | 3.1 mm | 4.0 mm |
|---|---|---|---|---|---|---|
| III | 100 mm | GE613R | GE614R | GE615R | GE616R | GE617R |
| XLI | 130 mm | | GE714R | | GE716R | GE717R |

**Neuro cutter**

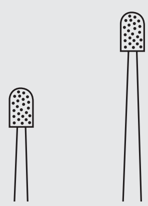

| | length | 3.1 mm | 3.1 mm |
|---|---|---|---|
| III | 100 mm | GE654R | GE655R |

For more power devices and drills, see "power systems" catalogue O22711 or O17599.

# Full HD Camera

**PV440** Full HD Camera system consisting of CCU, camera head with cable and zoomcoupler


**Full HD**

Six times higher resolution than conventional standard cameras delivers crystal clear images of the highest quality (1920 x 1080 pixels, progressive scan).

**True life colours**

Groundbreaking new 3-chip technology provides impressive colour depth and brilliant red differentation.

**Lag free images**

The latest Full HD technology delivers lag free images, even with rapid camera movements.

**Revolutionary zoom**

The world's first 5x zoom in an endoscopy camera shows even the tiniest details in perfect HD quality.

**PV944** 23" Full HD flat panel display

**PV909** Monitor stand for PV944


**Widescreen viewing**

The 16:9 image format extends the field of vision and facilitates earlier instrument identification.

**Multispeciality**

Special modes optimize the camera settings to meet the high demands according to the surgical speciality.

**On screen display**

All relevant camera information is displayed briefly. So you have everything in view.

For more visual equipment, see "Endoscopy Catalogue" C46702.

# Visual Equipment

**OP930** AXeL 180

**Xenon Light Source**

| | |
|---|---|
| System | Xenon |
| Integrated Spare lamp | No |
| Lamp Output | 180 W |
| Lamp Voltage | 15 V/12 A |

**Accessories**

| | |
|---|---|
| **OP931** | Xenon replacement bulb<br>15 V/180 W |

**Adapter for Xenon light source:**

| | |
|---|---|
| **OP936** | Wolf |
| **OP937** | Olympus (Xenon) |
| **OP938** | ACMI |

**Light guide cables, autoclavable, diam. 4.8 mm:**

| | |
|---|---|
| **OP906** | Length: 180 cm |
| **OP913** | Length: 250 cm |
| **OP914** | Length: 350 cm |

**Light guide cables adapter for light source of other make:**

| | |
|---|---|
| **TE683R** | Olympus |
| **TE688R** | Olympus-Xenon |
| **TE684R** | Wolf |

**PV920** Eddy DVD

**Digital Documentation System**

| | |
|---|---|
| DVD System | DVD-R/-RW; DVD+R/+RW |
| Colour System | PAL, NTSC |
| Still image format | JPEG, Bitmap |
| Video format | MPEG-2 |
| Number of MPEG-2 compression rates | 3 (high quality, standard, long play) |
| Capturing of video sequence | On hard drive, DVD/CD, USB or network |
| Capturing still images during video recording | Yes |


**PV941**

**15" Flat panel display "Touch Screen"**

| | |
|---|---|
| Panel Quality | With resistive touch-panel |
| Viewable Diagonal (Inches) | 15 |
| Brightness (cd/m²) | 250 |
| Resolution (Pixel) | 1024 x 768 (XGA) |
| Viewing Angle Horizontal/Vertical | 160°/160° |

For more visual equipment, see "Endoscopy Catalogue" C46702.

# Recommended Set acc. to Prof. Robert Reisch

| | |
|---|---|
| FH615R, FH610R, FH611R, PE487A, PE507A | MINOP® TREND Transnasal Endoscopy system incl. handle, trocar and scopes |
| FA041R – FA047R | TREND pituitary curettes, dissectors, hooks, enucleators |
| FA060R – FA068R | TREND pituitary curettes, dissectors, hooks, enucleators |
| FF590B | NOIR® transsphenoidal speculum |
| OK090R | Self-retaining nasal speculum |
| FA076R | Antrum bone punch |
| FA069R – FA075R | Pituitary scissors and forceps |
| FF345R | Landolt tumor grasping forceps |
| FM156R – FM158R | Sensation micro forceps straight |
| GK801R | Bipolar coagulation forceps with slender jaws & active tip opening |
| GF432R | Suction cannula Fukushima design with curved instrument tip |

| | |
|---|---|
| FK906B – FK909B | Kerrison NOIR®, detachable with thin footplate, upwards |
| FK936R – FK939R | Kerrison, detachable with thin footplate, downwards |
| FM682R, FM702, FM722R | XS tube shaft instruments, scissors and forceps |
| FF168R | Flexible holding arm with mechanic fixation |
| GD670, GD676, GD672, GD671 | Microspeed UNI, highspeed drill system, incl. motor & foot pedal |
| GB758R, GB771R | Hi-Line XS handpiece, angled and extra-long for narrow and deep-seated drill work |
| GE613R – GE617R | Hi-Line XS diamond burrs |
| PV440, PV944 | Full HD camera and wide-screen monitor |
| OP930 | Xenon light source |
| PV920 | Digital documentation system EDDY-DVD |

# Aesculap Neurosurgery Product Brochures

## Aesculap Neurosurgery Main Catalogue

... with all neurosurgery products.


For more information see
**Brochure C20102**

## Aesculap Power Systems Catalogue 2008

... Aesculap is a pioneer in surgical power systems.


For more information see
**Brochure O22711**

## Aesculap Power Systems Burrs & Blades Catalogue 2008

... Here it is... the Aesculap tools catalogue.


For more information see
**Brochure O17599**

## Neuroendoscopic Equipment

... for cranial and spinal neuroendoscopy.

## Visual Equipment


... Imaging and Accessories for Minimal Invasive Surgery.

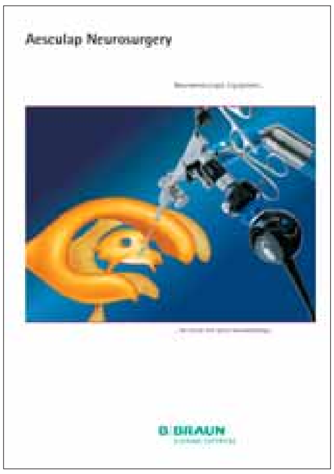


For more information see
**Brochure C35502**


For more information see
**Brochure C46702**

# Aesculap Academy

2005 FROST & SULLIVAN
2006 FROST & SULLIVAN
2007 FROST & SULLIVAN

**Global Medical Professional Education Institution of the Year Award**

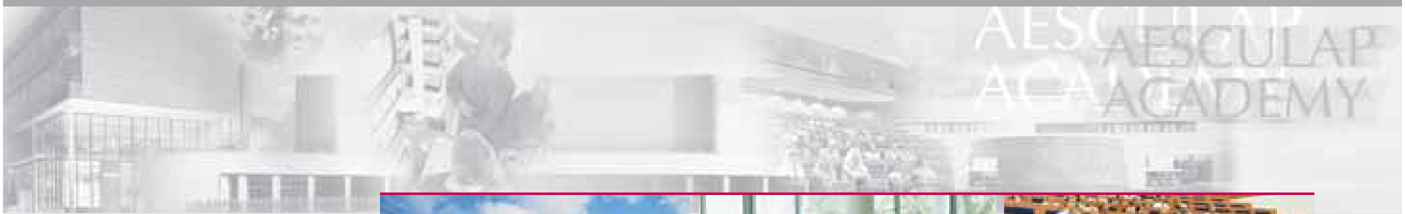


## **Horizons of Knowledge.** Competence to master the future.

AESCULAP AKADEMIE

Innovative developments in the field of medical technology, sophisticated new treatment methods, increasingly more stringent requirements or hospital and quality management and, last but not least, a healthy interest in acquiring new knowledge have given raise to an enormous and ver-increasing demand for further and advanced training.

The Aesculap Academy enjoys a world-wide reputation as a leading forum for basic and advanced training in the field medicine. The course program comprises a wide range of hands-on workshops, management
seminars and international symposia.

Aesculap Academy courses are of premium quality and are accredited by the espective medical societies and international medical organizations.

All of our courses are conducted by pioneering neurosurgeons who will address the theoretical knowledge of neuroendoscopy, cranial endoscopic anatomy, and clinical applications of neuroendoscopy. Each course includes extensive hands-on sessions or even live surgeries. Course attendees will benefit from discussions and analysis of real cases together with expert colleagues from all over the world. The training facilities of the Aesculap Academy in Berlin or Tuttlingen are traditional and spectacular locations for “sharing expertise”.

Competence to master the future – keep yourself fit for the future and ask for the latest course programme offerings, e.g.

- Basic Neuroendoscopy Courses
- Advanced Neuroendoscopy Courses
- Transnasal Pituitary & Skull Base Courses

**Visit our website and register for one of the next neuroendoscopy courses - www.aesculap-neuro.com or www.aesculap-academy.com, or contact your local B. Braun Aesculap representative.**

AESCULAP®

B|BRAUN
SHARING EXPERTISE

ISBN 978-3-00-025156-6

**Aesculap AG**

Am Aesculap-Platz
78532 Tuttlingen
Germany

Phone +49 7461 95-0
Fax +49 7461 95-2600

www.aesculap.de



Brochure No. C26402

0708/1.0/1